



Deposited via The University of Leeds.

White Rose Research Online URL for this paper:

<https://eprints.whiterose.ac.uk/id/eprint/149867/>

Version: Accepted Version

---

**Article:**

Liu, Y, Zhang, H, Men, H et al. (2019) Volume-regulated Cl<sup>-</sup> current: contributions of distinct Cl<sup>-</sup> channel and localized Ca<sup>2+</sup> signals. *American journal of physiology. Cell physiology*, 317 (3). C466-C480. ISSN: 0002-9513

<https://doi.org/10.1152/ajpcell.00507.2018>

---

© 2019, American Journal of Physiology-Cell Physiology. This is an author produced version of an article published in *Journal of Physiology-Cell Physiology*. Uploaded in accordance with the publisher's self-archiving policy.

**Reuse**

Items deposited in White Rose Research Online are protected by copyright, with all rights reserved unless indicated otherwise. They may be downloaded and/or printed for private study, or other acts as permitted by national copyright laws. The publisher or other rights holders may allow further reproduction and re-use of the full text version. This is indicated by the licence information on the White Rose Research Online record for the item.

**Takedown**

If you consider content in White Rose Research Online to be in breach of UK law, please notify us by emailing [eprints@whiterose.ac.uk](mailto:eprints@whiterose.ac.uk) including the URL of the record and the reason for the withdrawal request.

## **Volume-regulated Cl<sup>-</sup> current: contributions of distinct Cl<sup>-</sup> channel and localized Ca<sup>2+</sup> signals**

Yani Liu<sup>1,2</sup>, Huiran Zhang<sup>1,3</sup>, Hongchao Men<sup>1</sup>, Yuwei Du<sup>1</sup>, ZiqianXiao<sup>1</sup>, Fan Zhang<sup>1</sup>, Dongyang Huang<sup>1</sup>, Xiaona Du<sup>1</sup>, Nikita Gamper<sup>1,4</sup>, Hailin Zhang<sup>1\*</sup>

<sup>1</sup>Department of Pharmacology, Hebei Medical University; The Key Laboratory of Neural and Vascular Biology, Ministry of Education, China; The Key Laboratory of New Drug Pharmacology and Toxicology, Hebei Province; Shijiazhuang, China.

<sup>2</sup>Department of Pharmacology, School of Pharmacy, Qingdao University, Qingdao, Shandong, China.

<sup>3</sup>Department of Pulmonary Medicine, the Second Hospital of Hebei Medical University, Shijiazhuang, Hebei, China.

<sup>4</sup>School of Biomedical Sciences, Faculty of Biological Sciences, University of Leeds, Leeds, UK

\*Correspondence: Professor Hailin Zhang, Department of Pharmacology, Hebei Medical University, Shijiazhuang, China. 050017, E-mail: [zhanghl@hebmh.edu.cn](mailto:zhanghl@hebmh.edu.cn)

Running title: Volume-regulated chloride currents and intracellular Ca<sup>2+</sup> signals.

**Abbreviations:**

VRAC, volume regulated anion current

CaCC, calcium activated chloride channel

$I_{Cl,swell}$ , volume regulated chloride current

RVD, regulatory volume decreased

PLC, phospholipase C

EGTA, Ethylene glycol-bis ( $\beta$ -aminoethyl ether)-N,N,N',N'-tetraacetic acid

BAPTA, 1,2-Bis (2-amino-5- methylphenoxy) ethane-N,N,N',N'-tetraacetic acid

PIP<sub>2</sub>, phosphatidylinositol 4,5-bisphosphate

IP<sub>3</sub>, inositol 1,4,5-trisphosphate

DAG, 1,2-diacylglycerol

PKC, protein kinase C

BIM, Bisindolylmaleimide1

NFA, niflumic acid

DCPIB, 4-(2-Butyl-6,7-dichlor-2-cyclopentyl-indan-1-on-5-yl) oxybutyric acid

## Abstract

The swelling-activated chloride current ( $I_{Cl,swell}$ ) is induced when a cell swells and plays a central role in maintaining cell volume in response to osmotic stress. The major contributor of  $I_{Cl,swell}$  is the volume regulated anion channel (VRAC). LRRC8A (SWELL1) was recently identified as an essential component of VRAC but the mechanisms of VRAC activation are still largely unknown; moreover, other  $Cl^-$  channels, such as anoctamin 1 (ANO1) were also suggested to contribute to  $I_{Cl,swell}$ . In this present study, we investigated the roles of LRRC8A and ANO1 in activation of  $I_{Cl,swell}$ ; we also explored the role of intracellular  $Ca^{2+}$  in  $I_{Cl,swell}$  activation. We used CRISPR/Cas9 gene editing approach, electrophysiology, live fluorescent imaging, selective pharmacology and other approaches to show that both LRRC8A and ANO1 can be activated by cell swelling in HEK293 cells. Yet, both channels contribute biophysically and pharmacologically distinct components to  $I_{Cl,swell}$ , with LRRC8A being the major component. Cell swelling induced oscillatory  $Ca^{2+}$  transients and these  $Ca^{2+}$  signals were required to activate both, the LRRC8A- and ANO1-dependent components of  $I_{Cl,swell}$ . Both  $I_{Cl,swell}$  components required localized rather than global  $Ca^{2+}$  for activation. Interestingly, while intracellular  $Ca^{2+}$  was necessary and sufficient to activate ANO1, it was necessary but not sufficient to activate LRRC8A-mediated currents. Finally,  $Ca^{2+}$  transients linked to the  $I_{Cl,swell}$  activation were mediated by the GPCR-independent PLC isoforms.

Key words, volume regulated anion channel (VRAC),  $Ca^{2+}$  activated chloride channels (CaCCs), ANO1, LRRC8A,  $Ca^{2+}$

## Introduction

Volume regulated anion channel (VRAC) is widely expressed in most cell types; it mediates swelling activated Cl<sup>-</sup> currents ( $I_{Cl,swell}$ ), which are necessary for cell volume regulation. Being permeable to a range of organic and inorganic anions, VRAC plays many other important roles in cells, including proliferation, release of excitatory amino acids, apoptosis and germ cell development (21, 39, 45, 48). It is also suggested that VRAC is involved in a variety of human diseases, including stroke, diabetes and cancer (46, 52, 59). The molecular identity of VRAC remained unknown until recently, when the family of leucine-rich repeat containing 8 (LRRC8) proteins (also known as Swell) was identified as crucial components of VRAC (47, 57). LRRC8 family contains five members (LRRC8A-E), all of which share a high degree of sequence similarity (12). Whereas LRRC8A is the only obligatory subunit of VRAC, it still needs at least one of the other LRRC8 isoforms (57) to form a functional channel. The LRRC8 subunit composition determines not only biophysical properties of VRAC, such as inactivation kinetics and single channel conductance, but more importantly its substrate specificity (31, 46, 53, 55). Recently, the structures of LRRC8 family were determined by cryo-electron microscope and X-ray crystallography (12, 24). These reports revealed that VRAC is a hexameric protein with a modular structure.

However, it has to be noted that many other Cl<sup>-</sup> channels and transporters may also contribute to cell volume regulation. Notably, Ca<sup>2+</sup>-activated chloride channels ANO1, ANO6 and bestrophin were all reported to be involved in osmotic regulation (4, 6, 15, 25, 34, 44).

ANO1 (anoctamin-1), also known as TMEM16A, is the Ca<sup>2+</sup> activated chloride channel (CaCC) of the anoctamin family (ANO1-10) (8, 50, 58). Recent studies indicate that three anoctamin family members (ANO1, 6, and 10) may be involved in cell volume regulation (4, 18, 42). Thus, freshly isolated tissues from the ANO1, ANO6, or ANO10 knock-out mice show reduced regulatory volume decrease (RVD)

(4, 18, 42). It is, however, not clear whether these anoctamin proteins affect cell volume directly by acting as Cl<sup>-</sup> channels, or indirectly by contributing to Ca<sup>2+</sup> signaling (23, 49). In addition, another CaCC, bestrophin1, was also shown to be crucial for regulation of cell volume in mouse sperm and human retinal pigment epithelium cells (34).

The mechanism of I<sub>Cl,swell</sub> activation has long been debated; it is also not entirely clear whether the LRRC8-mediated VRAC is the sole contributor of I<sub>Cl,swell</sub> (2, 20, 41). Many cellular signaling cascades have been suggested to participate in the VRAC activation mechanism and among these the contribution of intracellular Ca<sup>2+</sup> signaling has been discussed frequently because cell swelling usually is accompanied by rises in the intracellular Ca<sup>2+</sup> concentration ([Ca<sup>2+</sup>]<sub>i</sub>) in many cell types (1-3, 37). It was also suggested that local Ca<sup>2+</sup> signals are probably also required for activation of VRAC (5). Yet, the exact role of Ca<sup>2+</sup> in activation of VRAC is not clear.

As mentioned, ANO1 channels were also reported to contribute to I<sub>Cl,swell</sub> (4); moreover, it was ported that ANO1 is activated by an increase in compartmentalized Ca<sup>2+</sup> (23, 26), hence, we set out to investigate roles of LRRC8A and ANO1 in I<sub>Cl,swell</sub> activation and test the potential role of Ca<sup>2+</sup> in activation of LRRC8A- and ANO1-mediated components of I<sub>Cl,swell</sub>. We also tested if source of intracellular Ca<sup>2+</sup> matters for the activation of VRAC or I<sub>Cl,swell</sub>. In this work we use the following terms to define closely related but distinct phenomena: *i*) term I<sub>Cl,swell</sub> is used to denote swelling-activated Cl<sup>-</sup> current, independent of its molecular identity; *ii*) term VRAC is used to denote volume regulated anion channel mediated by LRRC8 proteins; *iii*) term CaCC is used to denote Ca<sup>2+</sup>-activated Cl<sup>-</sup> channels.

## **Materials and methods**

### **Cell culture**

HEK293/CHO cells were cultured in DMEM/F12K with 10% fetal bovine serum

(FBS) and 1% penicillin/streptomycin at 37°C in a humidified atmosphere of air with 5% CO<sub>2</sub>. The ANO1 stably transfected HEK293 cells were established in our laboratory (30) and were cultured in DMEM supplemented with 10% FBS, 600 µg/ml G418 and 1% penicillin/streptomycin. DRG neurons were extracted from all spinal levels of 21-day-old Wistar rats, and neurons were dissociated and cultured as described (28). No growth factors were added to the culture medium (DMEM supplemented with GlutaMAX I (Invitrogen), 10% FBS and 1% penicillin/streptomycin). For the patch-clamp analysis cells were removed from the culture flask by a 1-min digestion with 2.5 mg/ml trypsin (1:250) and plated at low density onto 12-mm-diameter glass coverslips in 24-well tissue culture plates. The cells were used for recording within 48 h after plating.

### **cDNA and Transfection**

The mouse *ANO1* cDNA clone was kindly provided by Prof. Uhtaek Oh (Seoul National University, Korea) and was subcloned to expression vector pEGFPN1. The human *LRRC8A* cDNA clone was kindly provided by Prof. Thomas J. Jentsch (Neurocure, Charité Universitätsmedizin, Berlin, Germany). The *LRRC8A* knockout HEK293 (*LRRC8A*<sup>-/-</sup>) cells were transfected with above channel DNA constructs for 4-6 h with Lipofectamine 2000 (Invitrogen, USA) according to the manufacturer's instructions. The cells were used for patch-clamp recording 24 h after transfection.

### **CRISPR/Cas9 approach**

The ANO1 and *LRRC8A* knockout HEK293 cells were established using CRISPR/Cas9 approach (Beijing Biocytogen Co., Ltd., Beijing, China) and were cultured in DMEM with 10% FBS and 1% penicillin/streptomycin. To generate the knockout cell lines, pCS-sgRNA plasmids and targeting vector were co-electroporated into HEK293 cell line. After Electroporation, cells were treated with 1 µg/mL puromycin for 10 days. And then, resistant clones were picked and expanded for genotyping.

For detection of positive ANO1 and *LRRC8A* knockout HEK293 cell line clones, the

following primers were designed:	ANO1-GT-F:
5'-TGGGCCAGCATTAGATGAAGCAGTT-3',	PGK-GT-R:
5'-AGAAAGCGAAGGAGCAAAGCTGCTA-3',	ANO1-MSD-F:
5'-GAGGGCTTCAGAAAAGCAGAGAGCA-3',	ANO1-MSD-R:
5'-GGCTTGCGTGAGGTTTCATGTGTA-3'.	LRRC8A-GT-F:
5'-GTGATCACCCAGTTTGTGAGGGAGG-3',	LRRC8A-MSD-F:
5'-AGGAGTTCCCGATTGCTCTTACTGG-3',	LRRC8A-MSD-R:
5'-TGCAGTCGGTTCTCATAGCACACAG-3'.	

The primers ANO1-GT-F/PGK-GT-R, ANO1-MSD-F/ANO1-MSD-R; LRRC8A-GT-F/PGK-GT-R and LRRC8A-MSD-F/LRRC8A-MSD-R were respectively used to detect HR and non-HR allele.

### **Electrophysiology**

Currents were recorded using a MultiClamp 700B amplifier and pCLAMP 10.0 software (Molecular Devices, Sunnyvale, CA) and were filtered at 2 kHz. Patch electrodes with resistances of 2-5M $\Omega$  were pulled with a horizontal micropipette puller (P-97, Sutter Instruments, USA) and fire polished. The intracellular recording pipette solutions include: (1) the high Ca<sup>2+</sup> pipette solution (in mM)(30): 130 CsCl, 10 EGTA, 1 MgCl<sub>2</sub>, 10 HEPES, 2 Mg-ATP, 8 CaCl<sub>2</sub> (447 nM free Ca<sup>2+</sup>, calculated with the MAXC program, Stanford University, Stanford, CA, USA); pH adjusted to 7.3 with CsOH. (2) The hypertonic pipette solution (in mM): 140 CsCl, 2.4 MgCl<sub>2</sub>, 0.5 CaCl<sub>2</sub>, 5 EGTA, 10 HEPES, 5 Mg-ATP and 0.5 Na-GTP; pH 7.3 adjusted with CsOH; osmolality adjusted to 420 mOsm with sucrose. (3) The isosmotic pipette solution (in mM): 130 CsCl, 2.4 MgCl<sub>2</sub>, 0.5 CaCl<sub>2</sub>, 5 EGTA, 10 HEPES, 5 Mg-ATP and 0.5 Na-GTP; pH 7.3 adjusted with CsOH; osmolality adjusted to 320 mOsm with sucrose. The extracellular recording bath solutions include: ① the isosmotic bath solution (in mM): 145 NaCl, 2 CaCl<sub>2</sub>, 2 MgCl<sub>2</sub>, 10 Glucose, 10 HEPES; pH 7.4 adjusted with NaOH; osmolality adjusted to 320 mOsm with sucrose. ② The isosmotic bath solution (in mM) : 95 NaCl, 100 mannitol, 0.4 KH<sub>2</sub>PO<sub>4</sub>, 1.6 K<sub>2</sub>HPO<sub>4</sub>, 6 D-glucose, 1

MgCl<sub>2</sub>, 2 CaCl<sub>2</sub>; pH 7.4 adjusted with NaOH; osmolality adjusted to 320 mOsm with sucrose. ③ The hypotonic bath solution (in mM): 95 NaCl, 0.4 KH<sub>2</sub>PO<sub>4</sub>, 1.6 K<sub>2</sub>HPO<sub>4</sub>, 6 D-glucose, 1 MgCl<sub>2</sub>, 2 CaCl<sub>2</sub>; pH 7.4 adjusted with NaOH; osmolality adjusted to 220 mOsm with sucrose (this hypotonic bath solution is paired to the isosmotic bath solution ② and isosmotic pipette solution (3)). All recording were performed at room temperature.

### **Intracellular Ca<sup>2+</sup> imaging**

HEK293 cells were grown on glass coverslips and cultured for 24 h. For Ca<sup>2+</sup>-sensitive fluorescence detection, cells were loaded with Fluo-4-AM (2 μM) in the presence of Pluronic F-127 (0.02%) for 45 min at 37°C and the coverslips were placed into a flow-through chamber and mounted on an inverted microscope for confocal imaging. A Leica SP5 (Nussloch, Germany) DM-IRBE inverted microscope with a 20× objective (numerical aperture, 0.7) and a TCS-SP5 scan-head was used. The Fluo-4 was excited at 488 nm and the emitted fluorescence signal was detected at 520 nm. A time-laps series of confocal images were taken at 2 s intervals and were stored on a computer hard drive. Laser intensity and pinhole settings were kept constant between the experiments. The pinhole diameter was set to scan sections with a thickness of 0.28 μm. Control images were obtained for 2-5 min before test solution application. Hypotonic bath solution was applied for at least 20 min. TCS-SP5 confocal software (Leica) was used to analyze data off line.

### **Chemicals**

NFA, DCPIB, CaCC<sub>inh</sub>-A01, Thapsigargin, U73122 , U73343 , GDP-βs , Bisindolylmaleimide1 (BIM) and GTP-γS were purchased from Sigma (St Louis, MO, USA). These compounds were dissolved in DMSO and were kept at -20°C. Stock solutions were diluted to final concentrations in bath solution or intracellular solution. The final concentration of DMSO in bath solution or intracellular solution is no more than 0.1%. The vehicle at the final concentrations was tested and found having not effect on the currents measured. All final drug solutions were freshly made before

each experiment and kept away from light.

### **Data analysis and statistics**

The summary statistics of current densities were measured at -60 mV or +100 mV when the currents reached the maximum (oscillation) or relatively stable (no oscillation). Results were expressed as means  $\pm$  S.E.M. Student's test (unpaired and paired) and one-way ANOVA were used to assess statistical significance. Difference between means was considered significant at  $P < 0.05$ . Concentration-response curves were fitted with the logistic equation:  $y = A_2 + (A_1 - A_2) / (1 + (x/x_0)^p)$ , where  $y$  is the response;  $A_1$  and  $A_2$  are the maximum and minimum response, respectively,  $x$  is the drug concentration, and  $p$  is the Hill coefficient.

## **Results**

### **Localized intracellular $\text{Ca}^{2+}$ plays an essential role in activation of $I_{\text{Cl,swell}}$**

We first examined activation of  $I_{\text{Cl,swell}}$  by cell swelling in HEK293 cells (Fig. 1). An outwardly rectifying current gradually developed when the whole-cell currents were recorded using a hypertonic (420 mOsm) pipette solution in HEK293 cells. This current showed fast activation and slow inactivation at the highly positive voltages and could be inhibited by  $\text{Cl}^-$  channel blockers DCPIB (10  $\mu\text{M}$ ) (Fig. 1A) and  $\text{CaCC}_{\text{inh}}\text{-A01}$  (100  $\mu\text{M}$ , data not shown). In most cases, oscillations of the current amplitude were seen (Fig. 1A).

It has been suggested that intracellular  $\text{Ca}^{2+}$  is an important component in activation of swelling-induced currents (20, 22). To investigate the role of intracellular  $\text{Ca}^{2+}$  in activation of  $I_{\text{Cl,swell}}$ , we tested the effects of two  $\text{Ca}^{2+}$  chelators: Ethylene glycol-bis ( $\beta$ -aminoethyl ether)- $\text{N,N,N',N'}$ -tetraacetic acid (EGTA) and 1,2-Bis (2-amino-5-methylphenoxy) ethane- $\text{N,N,N',N'}$ -tetraacetic acid (BAPTA), as well as thapsigargin, a blocker of sarco-endoplasmic reticulum  $\text{Ca}^{2+}$ -ATPase (SERCA) on the development of  $I_{\text{Cl,swell}}$ . BAPTA and EGTA have similar affinity for  $\text{Ca}^{2+}$  but have markedly different binding kinetics; BAPTA binds  $\text{Ca}^{2+}$  nearly 100-fold faster than EGTA (27,

35, 36). These two  $\text{Ca}^{2+}$  chelators are thus often used to distinguish between ‘local’ and ‘global’  $\text{Ca}^{2+}$  signals as highly localized, micro- or nano- domain  $\text{Ca}^{2+}$  signals are minimally affected by slow chelator EGTA but usually can be efficiently precipitated by BAPTA. In contrast, slower, global  $\text{Ca}^{2+}$  signals are well prevented by both EGTA and BAPTA (33). As shown in Fig. 1B and 1C, addition of 20 mM BAPTA greatly reduced the  $I_{\text{Cl,swell}}$  amplitude while 20 mM EGTA had no effect. When cells were pre-incubated with thapsigargin (2  $\mu\text{M}$ ; 15 min) and the recording of  $I_{\text{Cl,swell}}$  was performed (still in the presence of thapsigargin), the current was also abolished (Fig. 1B, lower panel and 1C). It is interesting to note that although EGTA did not affect the  $I_{\text{Cl,swell}}$  amplitude, the oscillation of  $I_{\text{Cl,swell}}$  was not observed any more in the presence of EGTA (Fig. 1B; 0/14 recordings in the presence of 20 mM EGTA displayed oscillations vs. 26/26 recordings in the control condition with 5 mM EGTA). This similar effects of EGTA and BAPTA on  $I_{\text{Cl,swell}}$  were also observed in another two cell types: CHO cells (CHO-ANO1) and rat dorsal root ganglion neurons (Fig. 1D and 1E).

In another series of experiments we used a hypotonic extracellular bath solution (220 mOsm) instead of a hypertonic pipette solution (420 mOsm) to induce cell swelling. The hypotonic bath solution induced activation of  $I_{\text{Cl,swell}}$  with similar properties and amplitudes as the hypertonic pipette solution (Fig. 2A and 2E). Sensitivity of  $I_{\text{Cl,swell}}$  induced by extracellular hypotonicity to EGTA and BAPTA was similar to that observed for  $I_{\text{Cl,swell}}$  induced by hypertonic intracellular solution: 20 mM EGTA in the pipette solution had no effect, while 20 mM BAPTA almost completely abolished these currents (Fig. 2B and 2F). In addition, we also investigated the effect of extracellular  $\text{Ca}^{2+}$  on  $I_{\text{Cl,swell}}$  and the results showed that chelation of extracellular  $\text{Ca}^{2+}$  had no obvious effect on  $I_{\text{Cl,swell}}$  (Fig. 2A, lower panel and 2E).

We next studied if the osmotic cell swelling would indeed induce a rise in intracellular  $\text{Ca}^{2+}$ , as has been reported (20, 22). The hypotonic bath solution induced transient  $\text{Ca}^{2+}$  rises in all the HEK293 cells tested (Fig. 2C, shown are the time courses of fluorescence intensity changes from randomly selected three cells indicated by white

arrows). Similar to the  $I_{Cl,swell}$ , in most of the cells the  $Ca^{2+}$  transients were oscillating (Fig. 2C, left panel). To evaluate temporal correlation between the  $I_{Cl,swell}$  and  $Ca^{2+}$  oscillations we calculated and compared the intervals between the first and second peaks of  $I_{Cl,swell}$  and between the maxima of the first two  $Ca^{2+}$  transients. These intervals were  $9.7 \pm 0.9$  min (n=18) and  $4.7 \pm 0.4$  min (n=25), respectively, suggesting that the  $I_{Cl,swell}$  oscillations were significantly slower than  $Ca^{2+}$  oscillation. Interestingly, chelation of extracellular  $Ca^{2+}$  did not prevent swelling-induced  $Ca^{2+}$  transients (Fig. 2D and 2G); this effect was similar to the lack of effect of extracellular  $Ca^{2+}$  removal on  $I_{Cl,swell}$ .

As reported (47, 57), LRRC8A is an obligatory contributor of VRAC. To confirm its role in  $I_{Cl,swell}$ , we deleted LRRC8A (*LRRC8A*<sup>-/-</sup>) in HEK293 cells using CRISPR/Cas9 approach. As expected,  $I_{Cl,swell}$  in *LRRC8A*<sup>-/-</sup> HEK293 cells was dramatically reduced (Fig. 3A, top panel). Exogenous over-expression of LRRC8A into *LRRC8A*<sup>-/-</sup> HEK293 cells rescued the  $I_{Cl,swell}$  (Fig. 3A, bottom panel and 3C). These results confirm that LRRC8A-mediated VRAC is a major component of  $I_{Cl,swell}$  in HEK293 cells. We also tested the effects of EGTA, BAPTA and thapsigargin on the exogenously expressed LRRC8A currents. In *LRRC8A*<sup>-/-</sup> HEK293 cells re-transfected with LRRC8A, 20 mM EGTA in the pipette solution reduced the  $I_{Cl,swell}$  currents, and 20 mM BAPTA almost abolished the  $I_{Cl,swell}$  currents (Fig. 3B and 3D). Thus the  $I_{Cl,swell}$  produced by exogenously expressed LRRC8A is more sensitive to the  $Ca^{2+}$  chelators. Nonetheless, even in this case BAPTA and thapsigargin were significantly more potent than EGTA in inhibiting the  $I_{Cl,swell}$  currents (Fig. 3B and 3D).

We then tested if  $I_{Cl,swell}$  could be directly activated by elevated intracellular  $Ca^{2+}$ . Dialysis of 'high- $Ca^{2+}$ ' pipette solution (free  $[Ca^{2+}]_i = 447$  nM) under isotonic conditions was unable to activate  $I_{Cl,swell}$ -like currents either in the WT HEK293 cells or in *LRRC8A*<sup>-/-</sup> HEK293 cells transfected with LRRC8A (Fig. 4A, 4B, and 4D). To confirm that the dialysis of  $Ca^{2+}$  through the pipette in our experimental settings is effective, we used ANO1 as a  $Ca^{2+}$  sensor. In accord with our previous findings (30), the  $Ca^{2+}$ -activated-chloride currents (CaCC) through ANO1 were activated when the

WT HEK293 cells transfected with ANO1 were recorded with an isotonic pipette solution containing high-Ca<sup>2+</sup> solution (447 nM; Fig. 4C).

Taking together, the results presented in this section indicate that the Ca<sup>2+</sup> released from the intracellular Ca<sup>2+</sup> stores is an essential component in activation of LRRC8A-dependent I<sub>Cl,swell</sub>; the Ca<sup>2+</sup> signals necessary for the LRRC8A-dependent I<sub>Cl,swell</sub> activation are local in nature, whereas ‘global’ cytosolic Ca<sup>2+</sup> elevation does not activate the I<sub>Cl,swell</sub>/LRRC8A directly.

### **CaCC/ANO1 channels are also activated by the osmotic cell swelling.**

Thus far we have established that Ca<sup>2+</sup> is necessary for the activation of LRRC8A-dependent I<sub>Cl,swell</sub>. On the other hand, the CaCC/ANO1 channels were also implicated in the I<sub>Cl,swell</sub> (5, 6). Thus, we next tested the contribution of CaCC/ANO1 to the I<sub>Cl,swell</sub> activation under our experimental conditions. It was reported that HEK293 cells express low levels of endogenous ANO1 (4), thus, in order to rigorously test if ANO1 contributes to I<sub>Cl,swell</sub> in HEK293 cells, we first established a HEK293 cell line with deletion of ANO1 (*ANO1*<sup>-/-</sup>) using CRISPR/Cas9 approach. The I<sub>Cl,swell</sub> induced by the hypertonic pipette solution in *ANO1*<sup>-/-</sup> HEK293 cells was significantly reduced (Fig. 5A and 5D). When ANO1 was overexpressed in WT HEK293 cells (HEK293-ANO1), the I<sub>Cl,swell</sub> was significantly increased as compared to that in WT HEK293 cells (Fig. 5B and 5D). We also overexpressed ANO1 in *LRRC8A*<sup>-/-</sup> HEK293 cells (*LRRC8A*<sup>-/-</sup> + ANO1). In this case, in the absence of LRRC8A, cell swelling induced by the hypertonic pipette solution activated a large outwardly rectifying current (Fig. 5C and 5E).

Of note, altering levels of LRRC8A and ANO1 expression in HEK293 cells significantly affected swelling-induced I<sub>Cl,swell</sub> kinetics (Fig. 5A and 5B, right panels and Table 1). In the absence of ANO1 (*ANO1*<sup>-/-</sup> HEK293 cells, Fig. 5A), I<sub>Cl,swell</sub> displayed fast activation and prominent inactivation at more positive potentials; the inactivation was much more pronounced than that when the ANO1 was present (*cf.* Fig. 1A, bottom panel and 5A, right panel; see also Table 1). We assume that under

these conditions  $I_{Cl,swell}$  is mainly conducted by LRRC8 channels. In the absence of LRRC8A (*LRRC8A*<sup>-/-</sup> + ANO1, Fig. 5C) on the other hand,  $I_{Cl,swell}$  showed much slower activation and no inactivation. Under these conditions the  $I_{Cl,swell}$  is likely to be mostly conducted by ANO1. Cells in which both LRCC8A and ANO1 were present at the endogenous levels show  $I_{Cl,swell}$  with intermediate kinetics (Fig. 1A and Table 1); higher levels of LRCC8A resulted in increased inactivation (Fig. 3A, bottom panel and Table 1) while higher levels of ANO1 resulted in appearance of slowly activating component and disappearance of inactivation (Fig. 5C and Table 1). Contribution of ANO1 to  $I_{Cl,swell}$  was also further confirmed when  $I_{Cl,swell}$  was activated by an extracellular hypotonic solution in *LRRC8A*<sup>-/-</sup> HEK293 cells transfected with ANO1 (data not shown).

Adding further evidence that both LRRC8A and ANO1 contribute to  $I_{Cl,swell}$ , a Cl<sup>-</sup> current in HEK293 was induced by GTP- $\gamma$ S intracellularly applied under an isotonic condition (Fig. 5F-5H). Activation by GTP- $\gamma$ S is a hallmark of  $I_{Cl,swell}$  (38). Again, as in the case of the swelling-activated current, the GTP- $\gamma$ S-induced current in WT HEK293 cells displayed inactivation at strong depolarization (Fig. 5F) but when LRCC8A was deleted and ANO1 overexpressed, the GTP- $\gamma$ S-induced current became slowly-activating and lost its inactivation (Fig. 5G).

Taking together, the results shown in Fig. 1, 3 and 5 clearly demonstrate that endogenous LRRC8A and ANO1 proteins both contribute to the  $I_{Cl,swell}$ , although LRCC8A is being the dominant component. Exogenously expressed ANO1 as well as LRRC8A could also be activated by cell swelling.

In light of our findings that intracellular Ca<sup>2+</sup> is an essential but not a sufficient factor in activation of  $I_{Cl,swell}$  during the cell swelling, and that intracellular Ca<sup>2+</sup> is sufficient to directly activate ANO1, which, in turn, can also be activated by cell swelling, we hypothesized that ANO1 could act as the Ca<sup>2+</sup> sensor for LRRC8A activation. In support to this hypothesis is the fact that LRRC8A and ANO1 were reported to interact directly (5). Thus, we tested the Ca<sup>2+</sup> dependency of  $I_{Cl,swell}$  activation in the

absence of ANO1. Similar to the activation of  $I_{Cl,swell}$  in the presence of both LRRC8A and ANO1 (WT HEK293 cells), activation of  $I_{Cl,swell}$  in the absence of ANO1 (*ANO1*<sup>-/-</sup> cells) was still inhibited by BAPTA but not by EGTA added to the hypertonic pipette solution (Fig. 6A, 6B and 6E). This result indicates that the dependence of the  $I_{Cl,swell}$  activation from local  $Ca^{2+}$  does not require ANO1. We also tested if deletion of either LRRC8A or ANO1 would affect the swelling-induced rises in intracellular  $Ca^{2+}$ , which was not the case (Fig. 6C, 6D and 6F). Likewise, chelation of extracellular  $Ca^{2+}$  did not prevent swelling-induced  $Ca^{2+}$  transients (Fig. 6C, 6D and 6F).

### **Pharmacological characterization of $I_{Cl,swell}$**

The results presented above suggested that both LRRC8A and ANO1 could be activated by the cell swelling but these channels generate currents with different kinetics. We next studied if these two types of chloride currents have different sensitivity to pharmacological modulators of chloride channels and thus could be isolated pharmacologically. For this, we compared effects of two drugs: niflumic acid (NFA) and 4-(2-Butyl-6,7-dichlor-2-cyclopentyl-indan-1-on-5-yl) oxybutyric acid (DCPIB). NFA is a broad spectrum chloride channel inhibitor and our previous study shows that NFA has higher selectivity towards ANO1 as compared to another CaCC, Bestrophin 1 (30). DCPIB has been reported as a selective VRAC blocker (11, 16), but its effect on ANO1 has not been systematically tested. These two drugs were tested for their effects on three different current types: *i*)  $I_{Cl,swell}$  from WT HEK293 cells ( $I_{Cl,swell}$ ) induced with 420 mOsm pipette solution; *ii*)  $I_{Cl,swell}$  from ANO1-stably expressed HEK293 cells ( $I_{Cl,swell} + ANO1$ ) induced with 420 mOsm pipette solution; and *iii*) CaCC current from ANO1-stably expressed HEK293 cells (CaCC/ANO1) induced with the isotonic pipette solution supplemented with 447 nM free  $Ca^{2+}$ . Examples of whole-cell current traces recorded in these three different conditions and the effects of two drugs are shown in Fig. 7. The concentration dependencies for both compounds are analyzed in Fig. 7C and 7D, and summarized in Table 2. NFA inhibited three types of current (measured at +100 mV) with potency ( $IC_{50}$ ) order of: CaCC/ANO1 ( $3.35 \pm 1.87 \mu M$ ) >  $I_{Cl,swell} + ANO1$  ( $95.8 \pm 15.6 \mu M$ ) >  $I_{Cl,swell}$  ( $471.4 \pm$

132.8  $\mu\text{M}$ ). On the contrary, the sensitivity of the three currents to DCPIB had an inverted sequence:  $I_{\text{Cl,swel}}$  ( $5.69 \pm 1.60 \mu\text{M}$ )  $\sim$   $I_{\text{Cl,swel}} + \text{ANO1}$  ( $7.04 \pm 2.29 \mu\text{M}$ )  $>$  CaCC/ANO1 ( $18.8 \pm 2.71 \mu\text{M}$ ). We also tested the sensitivity of the three types of currents to NFA and DCPIB at -60 mV and obtained the same orders of sensitivity as at +100 mV (Table 2).

NFA-sensitive component of  $I_{\text{Cl,swel}} + \text{ANO1}$  gave rise to a very characteristic, slowly activating and non-inactivation current similar to these of ANO1-mediated CaCC (*cf.* Fig. 7B, top and 5C). On the contrary, the DCPIB-sensitive component of  $I_{\text{Cl,swel}} + \text{ANO1}$  gave rise to the current with fast activation and inactivation, characteristic for the LRRC8A-mediated  $I_{\text{Cl,swel}}$  (*cf.* Fig. 7B, bottom and 5A). Collectively, these results clearly indicate that in HEK293 cells swelling-activated  $I_{\text{Cl,swel}} + \text{ANO1}$  has at least two components, mediated by LRRC8A and ANO1; these components have distinct kinetics and pharmacology.

### **Probing cell signaling mechanisms for $\text{Ca}^{2+}$ involvement in the activation of $I_{\text{Cl,swel}}$**

Since cell swelling-induced  $\text{Ca}^{2+}$  transients did not require extracellular  $\text{Ca}^{2+}$ , we concluded that in this case  $\text{Ca}^{2+}$  is being released from the intracellular stores. One common signaling pathway for such intracellular  $\text{Ca}^{2+}$  transients is through phospholipase (PLC) mediated  $\text{Ca}^{2+}$  release from the endoplasmic reticulum  $\text{Ca}^{2+}$  stores. Thus, we first tested the role of PLC in the activation of  $I_{\text{Cl,swel}}$ , as was suggested in previous studies (9, 13, 60). PLC inhibitor U73122 (5  $\mu\text{M}$ ) almost completely blocked the activation of  $I_{\text{Cl,swel}}$  (Fig. 8A, top and 8B), an effect that was not observed with the inactive analogue, U73343 (5  $\mu\text{M}$ ) (Fig. 8A, bottom and 8B). We then synthesized a series of siRNAs against the PLC isoforms which are known to be highly expressed in HEK293 cells (“THE HUMAN PROTEIN ATLAS” database):  $\text{PLC}_{\gamma 1}$ ,  $\text{PLC}_{\beta 3 \& 4}$ ,  $\text{PLC}_{\delta 3}$  and  $\text{PLC}_{\epsilon 1}$ . These siRNAs were individually transfected into the HEK293 cells and their efficiency in inhibiting the activation of  $I_{\text{Cl,swel}}$  was tested. Among five PLC isoforms tested, knockdown of  $\text{PLC}_{\gamma 1}$ ,  $\text{PLC}_{\beta 3}$  or  $\text{PLC}_{\delta 3}$  reduced the

activated  $I_{Cl,swell}$  significantly, whereas the knockdown of  $PLC_{\beta 4}$  and  $PLC_{\epsilon 1}$  had no effect (Fig. 8D). Taking together, these results indicate PLC isoforms were indeed involved in activation of  $I_{Cl,swell}$ .

PLC hydrolyzes the plasma membrane phospholipid, phosphatidylinositol 4,5-bisphosphate ( $PIP_2$ ) into inositol 1,4,5-trisphosphate ( $IP_3$ ) and 1,2-diacylglycerol (DAG), which in turn, results in the mobilization of intracellular  $Ca^{2+}$  and the activation of protein kinase C (PKC), respectively. We, thus, tested if the substrate of PLC,  $PIP_2$  is involved in the activation of  $I_{Cl,swell}$ . In the first series of experiments, we transfected HEK293 cells with  $PLC\delta$ -PH-GFP, a fluorescent probe containing the  $PIP_2$ -binding domain from  $PLC\delta$  fused to GFP. This probe binds to  $PIP_2$  (51) and  $IP_3$  (for which the probe has higher affinity (19, 29, 56)). Using  $PLC\delta$ -PH-GFP as an optical probe for  $PIP_2$  hydrolysis, we could not detect a clear depletion of membrane of  $PIP_2$  under a condition of cell swelling (Data not shown).

We next examined the effect of G-protein blocker GDP- $\beta$ s (500  $\mu$ M) and PKC inhibitor bisindolylmaleimide (BIM 200 nM) on the  $I_{Cl,swell}$  activation; no obvious effects of either of these compounds on the activation of  $I_{Cl,swell}$  were observed (Data not shown). Taken together these data suggest that while the  $Ca^{2+}$  required for the  $I_{Cl,swell}$  activation is likely to be produced by the PLC activity, this activity is perhaps independent of the GPCR activation; indeed  $PLC\delta$  and  $\gamma$  isoforms are activated by  $Ca^{2+}$  and tyrosine kinases, respectively (17). In addition, this PLC activity is perhaps also highly localized as no global  $PIP_2$  depletion was observed.

## Discussion

In this study we investigated molecular correlates and activation mechanisms of  $I_{Cl,swell}$ . We report the following findings: *i*) LRRC8A and ANO1 can both be activated by cell swelling. *ii*) Both channels contribute biophysically and pharmacologically distinct components to the swelling-induced chloride currents in

HEK293 cells, with LRRC8A being the major component. *iii*) Both  $I_{Cl,swell}$  components require localized rather than global  $Ca^{2+}$  for activation. *iv*) While intracellular  $Ca^{2+}$  is necessary and sufficient to activate ANO1, it is necessary but not sufficient to activate LRRC8A-mediated currents. *v*)  $Ca^{2+}$  signals that are necessary for  $I_{Cl,swell}$  activation are mediated by the GPCR-independent PLC activation.

The molecular identity of currents constituting  $I_{Cl,swell}$ , including VRAC, remained controversial until 2014 when LRRC8A and its family members (LRRC8B-E) were shown to function as VRAC (47, 57). However, the other candidates such as ANO1, ANO6 and bestrophin1 were also proposed to contribute to  $I_{Cl,swell}$  in certain conditions (4, 6, 15, 34). Our results show that in LRRC8A knockout HEK293 (*LRRC8A*<sup>-/-</sup>) cells,  $I_{Cl,swell}$  was almost abolished. When LRRC8A was transfected into *LRRC8A*<sup>-/-</sup> cells,  $I_{Cl,swell}$  was rescued but with somewhat altered properties (no oscillations, reduced requirements for local  $Ca^{2+}$ ; see below), suggesting that exogenously expressed LRRC8A can recapitulate most but not all the properties of endogenous  $I_{Cl,swell}$ . The reason for such partial phenotype could be, for example, in different membrane localization of exogenous and endogenous LRRC8A.

In addition, our data clearly show that ANO1 can also generate  $I_{Cl,swell}$ , albeit, again, with some features which are clearly distinct from the endogenous  $I_{Cl,swell}$  (slow activation, no inactivation, stronger dependence on  $Ca^{2+}$ ). Specifically,  $I_{Cl,swell}$  was significantly reduced in *ANO1*<sup>-/-</sup> cells; in addition,  $I_{Cl,swell}$  was significantly increased in ANO1 overexpressed HEK293 cells, and even in *LRRC8A*<sup>-/-</sup> cells transfected with ANO1. Interestingly, it was reported that  $I_{Cl,swell}$  was strongly suppressed in HEK293 cells when LRRC8A was overexpressed and partially rescued in *LRRC8A*<sup>-/-</sup> cells re-transfected with LRRC8A (57). These authors hypothesized that LRRC8A is a part of a heteromeric VRAC and that LRRC8A overexpression leads to a subunit stoichiometry that is incompatible with normal channel activity. Here, we hypothesized ANO1 might be another key element of the VRAC complex, indeed a direct interaction between ANO1 and LRRC8A has been proposed (5). But how exactly ANO1 contributes to the VRAC activity is still unknown. The fact that

biophysically distinct ANO1-like and LRRC8A-like current fractions can be pharmacologically isolated from the macroscopic  $I_{Cl,swell}$  speaks against the formation of *bona fide* LRRC8A:ANO1 heteromeric channels with a common pore. Most likely both channels maintain independent pores and gating mechanisms. Yet, there is a remarkable level of coordination between two channels as both are activated by swelling and GDP $\gamma$ s and both require local  $Ca^{2+}$  signals.

Previous data from us and others suggest that ANO1 is endogenously expressed in HEK293 cells, although at much lower levels than LRRC8A (16, 57). Yet, WT HEK293 displays no obvious CaCC currents in electrophysiological experiments (Fig. 4A). One possibility to explain some of the observed results, including a lack of CaCC in WT HEK293 cells, is to hypothesize that under basal conditions the ion channels contributing to  $I_{Cl,swell}$  reside at the plasma membrane locations that are poorly accessible from cytosol. One example of such membrane structures is junctions between the plasma membrane and endoplasmic reticulum (ER-PM junctions). Recent studies indeed suggested a presence of ANO1 at such junctions (5, 10, 23, 26); it could be further hypothesized that VRAC channel complexes are also located at these or similar junctional domains. We further hypothesize that within these locations VRACs (and CaCCs) are very poorly accessible to ‘global’ cytosolic  $Ca^{2+}$  (e.g.  $Ca^{2+}$  dialyzed through the patch pipette). Cell swelling may induce *i*) mechanical rearrangements within the ER-PM junctions that expose the channels to cytosol and/or *ii*) increase in compartmentalized  $Ca^{2+}$  at the junctions. These events would expose ANO1 and LRRC8 channels to  $Ca^{2+}$  and, ultimately, result in the  $I_{Cl,swell}$  activation (5).

Indeed, both LRRC8A- and ANO1-mediated  $I_{Cl,swell}$  components required local  $Ca^{2+}$  for activation as the swelling-induced current was strongly reduced by BAPTA but not EGTA in WT HEK293 cells. Pretreatment of the cells with thapsigargin (ER store depletion) also strongly suppressed  $I_{Cl,swell}$ . Interestingly, when either LRRC8A or ANO1 were overexpressed, they become more sensitive to global  $Ca^{2+}$ : the current mediated by overexpressed LRRC8A became more sensitive to EGTA (Fig. 3B and

3D) while overexpressed (but not endogenous) ANO1 could be activated by dialysis of  $\text{Ca}^{2+}$  through the patch pipette (Fig. 4C). These data indirectly support the hypothesis that endogenous  $\text{Cl}^-$  channels contributing to  $I_{\text{Cl,swell}}$  are protected from global cytosolic  $\text{Ca}^{2+}$  and could only be activated by localized release of  $\text{Ca}^{2+}$  from the ER (e.g. upon cell swelling) while the overexpressed channels are much more open to global  $\text{Ca}^{2+}$  signals.

It has to be pointed out that the contribution of intracellular  $\text{Ca}^{2+}$  signaling to VRAC activation has been debated (2, 22). Many studies have demonstrated noticeable swelling-induced current even in the presence of high concentrations of  $\text{Ca}^{2+}$  chelators loaded into the cells or in the absence of observable  $[\text{Ca}^{2+}]_i$  rises in some cell types (2, 20, 40). These studies however could not rule out the requirements for highly localized  $\text{Ca}^{2+}$  signals reported here. Some reports have suggested the requirement of minimal basal  $[\text{Ca}^{2+}]_i$  (54). Akita and colleagues suggested that in cultured astrocytes, the swelling-induced activation of VRAC requires both,  $\text{Ca}^{2+}$ -dependent and  $\text{Ca}^{2+}$ -independent events. In line with this, a recent study showed that swelling induced taurine and glucose release mediated by VRAC exhibits both  $\text{Ca}^{2+}$ -dependent and -independent mechanisms, which was related to the different VRAC heteromers expressed in human retinal cell lines (MIO-M1) (37). Thus, while conflicting evidence exist,  $\text{Ca}^{2+}$  does seem to play an important role for at least some steps in VRAC activation.

How cell swelling is coupled to  $\text{Ca}^{2+}$  release from the ER is not entirely clear but our results show that in HEK293 cells both the swelling-induced  $\text{Ca}^{2+}$  transients and the  $I_{\text{Cl,swell}}$  activation require the PLC; this observation is supported by several earlier reports (9, 13, 60). We show that PLC inhibition (U73122) or down regulation (siRNA), or ER  $\text{Ca}^{2+}$  store depletion (thapsigargin), all significantly reduced or abolished  $I_{\text{Cl,swell}}$ . Yet, the GDP- $\beta$ S was unable to prevent swelling-induced  $I_{\text{Cl,swell}}$  activation and no obvious swelling-induced  $\text{PIP}_2$  depletion could be observed (Data not shown). Thus, exact mechanism by which swelling activates PLC and ER  $\text{Ca}^{2+}$  release remains to be solved; perhaps it relies mostly on the GPCR-independent PLC

isoforms, including PLC $_{\gamma 1}$  and PLC $_{\delta 3}$ .

In the study, oscillation of  $I_{Cl,swell}$  amplitude was always seen when the cells swell. When the hypertonic intracellular solution was dialyzed into HEK293 cells, or when cells were placed into the hypotonic extracellular solution, the cells began to swell and the  $I_{Cl,swell}$  started to develop. After reaching a maximum within several minutes, slow oscillations began; the first peak current was usually the largest. In some recordings these slow oscillations were observed for over an hour. Interestingly, the  $[Ca^{2+}]_i$  also displayed prominent oscillations, but this process had a significantly higher frequency: the times between first two peaks of  $I_{Cl,swell}$  and  $[Ca^{2+}]_i$  were calculated to be 9.7 and 4.7 min, respectively. If  $Ca^{2+}$  is required for  $I_{Cl,swell}$  activation, why the current and  $[Ca^{2+}]_i$  oscillations would not have the same kinetics? One potential explanation could be in that the kinetics of changes of local  $Ca^{2+}$  concentration in the immediate proximity of volume-sensitive  $Cl^-$  channel and the kinetics of global cytosolic  $[Ca^{2+}]_i$  measured with fluo-4 may not be the same. Indeed, as we hypothesized above, VRACs may reside in the areas that are, to a degree, restricted from the rest of the cytosol; hindered diffusion of  $Ca^{2+}$  into these locations may, therefore, slowdown  $Ca^{2+}$  dynamics, which, in turn, results in slower current oscillations. We also measured the intracellular  $Ca^{2+}$  transients coupled with  $I_{Cl,swell}$  measurement in patch clamped cells. In this case,  $[Ca^{2+}]_i$  oscillations were also observed and again no time-matched kinetics of  $[Ca^{2+}]_i$  and  $I_{Cl,swell}$  were strictly correlated (data not shown). Thus the  $Ca^{2+}$  kinetics accompanying  $I_{Cl,swell}$  is a complex issue which need to be studied in further investigations.

It is worthy to note that no oscillation of  $I_{Cl,swell}$  was reported before. We have some preliminary thoughts on why we are different with others on seeing such high proportion of  $I_{Cl,swell}$  oscillation. 1) The oscillation usually takes a slow start with an even slower oscillation cycle (e.g. Fig 1 and Fig 2). In the literature, VRAC was usually recorded within 15 min (5, 47, 57), whereas we recorded VRAC in a much longer period of time; in another word, the oscillation of VRAC was simply being missed in others' recordings. 2) It seems that the oscillation of VRAC was most often seen in  $I_{Cl,swell}$  induced by the

hypertonic pipette solution than  $I_{Cl,swell}$  induced by the hypotonic external solution which in most cases was used in others' experiments; in our case, 85% of 90 HEK293 cells recorded using the hypertonic pipette solution developed multiple oscillation, whereas only 33% of 27 HEK293 cells recorded using the hypotonic external solution developed oscillation with more than 2 cycles. It is of note that the frequencies encoded in  $Ca^{2+}$  oscillations are reported to regulate many cellular processes such as exocytosis (32), apoptosis (43), fertilization (7) and cell growth (14); now VRAC can also be added to this list. The phenomenon of  $I_{Cl,swell}$  oscillation and its relationships with the swelling-induced oscillations of  $[Ca^{2+}]_i$  is fascinating and requires further investigation.

In sum, here we show that both LRRC8A and ANO1 contribute to  $I_{Cl,swell}$  in HEK293 cells and that  $I_{Cl,swell}$  activation requires localized, PLC-mediated  $Ca^{2+}$  release from the ER. The exact nature of ANO1-LRRC8A interactions during the  $I_{Cl,swell}$  activation is still unknown; the fact that activation of  $I_{Cl,swell}$  in the absence of ANO1 (*ANO1*<sup>-/-</sup> cells) still required local  $Ca^{2+}$  (Fig. 5) indicates that ANO1 is unlikely to just simply play a role of a  $Ca^{2+}$  sensor for LRRC8A. Clearly, future research is needed to decipher exact relationships between cell swelling, PLC, intracellular  $Ca^{2+}$  transients, LRRC8A, ANO1, VRAC and  $I_{Cl,swell}$  activation.

**Acknowledgments** This work is supported by the National Natural Science Foundation of China (91732108 to HZ), (81500057 to HZ), (31571088 to XD), (31872788 to FZ), and (GZR81701113 to DH); Key Basic Research Project of Applied Basic Research Program of Hebei Province (16967712D to XD); Biotechnology and Biological Sciences Research Council (Grants BB/R003068/1 and BB/R02104X/1 to NG); Hebei Province Department of Education Grant (BJ2017004 to DH). We greatly appreciate the gift of mouse ANO1 cDNA from Prof. Uhtaek Oh (Seoul National University, Korea) and human LRRC8A cDNA clone was kindly provided by Prof. Thomas J. Jentsch (Neurocure, Charité Universitätsmedizin,

Germany).

**Author Contributions** YL, HuZ, HM, YD, ZX, DH and FZ performed the experiments and data analyses. YL, HuZ, XD, NG and HaZ designed the research. YL, NG and HaZ wrote the paper. All authors have read, commented and approved the content of the manuscript.

**Conflict of interest.** There are no conflicts of interest.

## References

1. **Akita, T., S.V. Fedorovich, and Y. Okada**, Ca<sup>2+</sup> nanodomain-mediated component of swelling-induced volume-sensitive outwardly rectifying anion current triggered by autocrine action of ATP in mouse astrocytes. *Cell Physiol Biochem.* 28(6): p. 1181-90, 2011.
2. **Akita, T. and Y. Okada**, Characteristics and roles of the volume-sensitive outwardly rectifying (VSOR) anion channel in the central nervous system. *Neuroscience.* 275: p. 211-31, 2014.
3. **Akita, T. and Y. Okada**, Regulation of bradykinin-induced activation of volume-sensitive outwardly rectifying anion channels by Ca<sup>2+</sup> nanodomains in mouse astrocytes. *J Physiol.* 589(Pt 16): p. 3909-27, 2011.
4. **Almaca, J., Y. Tian, F. Aldehni, J. Ousingsawat, P. Kongsuphol, J.R. Rock, B.D. Harfe, R. Schreiber, and K. Kunzelmann**, TMEM16 proteins produce volume-regulated chloride currents that are reduced in mice lacking TMEM16A. *J Biol Chem.* 284(42): p. 28571-8, 2009.
5. **Benedetto, R., L. Sirianant, I. Pankonien, P. Wanitchakool, J. Ousingsawat, I. Cabrita, R. Schreiber, M. Amaral, and K. Kunzelmann**, Relationship between TMEM16A/anoctamin 1 and LRRC8A. *Pflugers Arch.* 468(10): p. 1751-63, 2016.
6. **Bulley, S., Z.P. Neeb, S.K. Burris, J.P. Bannister, C.M. Thomas-Gatewood, W. Jangsangthong, and J.H. Jaggat**, TMEM16A/ANO1 channels contribute to the myogenic response in cerebral arteries. *Circ Res.* 111(8): p. 1027-36, 2012.
7. **Campbell, K. and K. Swann**, Ca<sup>2+</sup> oscillations stimulate an ATP increase during fertilization of mouse eggs. *Dev Biol.* 298(1): p. 225-33, 2006.
8. **Caputo, A., E. Caci, L. Ferrera, N. Pedemonte, C. Barsanti, E. Sondo, U. Pfeffer, R. Ravazzolo, O. Zegarra-Moran, and L.J. Galletta**, TMEM16A, a membrane protein associated with calcium-dependent chloride channel activity. *Science.* 322(5901): p. 590-4, 2008.
9. **Catacuzzeno, L., A. Michelucci, L. Sforza, F. Aiello, M. Sciacaluga, B. Fioretti, E. Castigli, and F. Franciolini**, Identification of key signaling molecules involved in the activation of the swelling-activated chloride current in human glioblastoma cells. *J Membr Biol.* 247(1): p. 45-55, 2014.
10. **Courjaret, R. and K. Machaca**, Mid-range Ca<sup>2+</sup> signalling mediated by functional coupling

- between store-operated Ca<sup>2+</sup> entry and IP<sub>3</sub>-dependent Ca<sup>2+</sup> release. *Nat Commun.* 5: p. 3916, 2014.
11. **Decher, N., H.J. Lang, B. Nilius, A. Bruggemann, A.E. Busch, and K. Steinmeyer**, DCPIB is a novel selective blocker of I(Cl,swell) and prevents swelling-induced shortening of guinea-pig atrial action potential duration. *Br J Pharmacol.* 134(7): p. 1467-79, 2001.
  12. **Deneka, D., M. Sawicka, A.K.M. Lam, C. Paulino, and R. Dutzler**, Structure of a volume-regulated anion channel of the LRRC8 family. *Nature.* 558(7709): p. 254-259, 2018.
  13. **Ellershaw, D.C., I.A. Greenwood, and W.A. Large**, Modulation of volume-sensitive chloride current by noradrenaline in rabbit portal vein myocytes. *J Physiol.* 542(Pt 2): p. 537-47, 2002.
  14. **Ferreira-Martins, J., C. Rondon-Clavo, D. Tugal, J.A. Korn, R. Rizzi, M.E. Padin-Iruegas, S. Ottolenghi, A. De Angelis, K. Urbanek, N. Ide-Iwata, D. D'Amario, T. Hosoda, A. Leri, J. Kajstura, P. Anversa, and M. Rota**, Spontaneous calcium oscillations regulate human cardiac progenitor cell growth. *Circ Res.* 105(8): p. 764-74, 2009.
  15. **Fischmeister, R. and H.C. Hartzell**, Volume sensitivity of the bestrophin family of chloride channels. *J Physiol.* 562(Pt 2): p. 477-91, 2005.
  16. **Friard, J., M. Tauc, M. Cougnon, V. Compan, C. Durantou, and I. Rubera**, Comparative Effects of Chloride Channel Inhibitors on LRRC8/VRAC-Mediated Chloride Conductance. *Front Pharmacol.* 8: p. 328, 2017.
  17. **Gresset, A., J. Sonddek, and T.K. Harden**, The phospholipase C isozymes and their regulation. *Subcell Biochem.* 58: p. 61-94, 2012.
  18. **Hammer, C., P. Wanitchakool, L. Sirianant, S. Papiol, M. Monnheim, D. Faria, J. Ousingsawat, N. Schramek, C. Schmitt, G. Margos, A. Michel, P. Kraiczky, M. Pawlita, R. Schreiber, T.F. Schulz, V. Fingerle, H. Tumani, H. Ehrenreich, and K. Kunzelmann**, A Coding Variant of ANO10, Affecting Volume Regulation of Macrophages, Is Associated with Borrelia Seropositivity. *Mol Med.* 21: p. 26-37, 2015.
  19. **Hirose, K., S. Kadowaki, M. Tanabe, H. Takeshima, and M. Iino**, Spatiotemporal dynamics of inositol 1,4,5-trisphosphate that underlies complex Ca<sup>2+</sup> mobilization patterns. *Science.* 284(5419): p. 1527-30, 1999.
  20. **Hoffmann, E.K., I.H. Lambert, and S.F. Pedersen**, Physiology of cell volume regulation in vertebrates. *Physiol Rev.* 89(1): p. 193-277, 2009.
  21. **Hyzinski-Garcia, M.C., A. Rudkouskaya, and A.A. Mongin**, LRRC8A protein is indispensable for swelling-activated and ATP-induced release of excitatory amino acids in rat astrocytes. *J Physiol.* 592(22): p. 4855-62, 2014.
  22. **Jentsch, T.J.**, VRACs and other ion channels and transporters in the regulation of cell volume and beyond. *Nat Rev Mol Cell Biol.* 17(5): p. 293-307, 2016.
  23. **Jin, X., S. Shah, Y. Liu, H. Zhang, M. Lees, Z. Fu, J.D. Lippiat, D.J. Beech, A. Sivaprasadarao, S.A. Baldwin, H. Zhang, and N. Gamper**, Activation of the Cl<sup>-</sup> channel ANO1 by localized calcium signals in nociceptive sensory neurons requires coupling with the IP<sub>3</sub> receptor. *Sci Signal.* 6(290): p. ra73, 2013.
  24. **Kefauver, J.M., K. Saotome, A.E. Dubin, J. Pallesen, C.A. Cottrell, S.M. Cahalan, Z. Qiu, G. Hong, C.S. Crowley, T. Whitwam, W.H. Lee, A.B. Ward, and A. Patapoutian**, Structure of the human volume regulated anion channel. *Elife.* 7, 2018.
  25. **Kunzelmann, K.**, TMEM16, LRRC8A, bestrophin: chloride channels controlled by Ca<sup>2+</sup>

- and cell volume. *Trends Biochem Sci.* 40(9): p. 535-43, 2015.
26. **Kunzelmann, K., I. Cabrita, P. Wanitchakool, J. Ousingsawat, L. Sirianant, R. Benedetto, and R. Schreiber,** Modulating Ca(2)(+) signals: a common theme for TMEM16, Ist2, and TMC. *Pflugers Arch.* 468(3): p. 475-90, 2016.
  27. **Lee, S.J., Y. Escobedo-Lozoya, E.M. Szatmari, and R. Yasuda,** Activation of CaMKII in single dendritic spines during long-term potentiation. *Nature.* 458(7236): p. 299-304, 2009.
  28. **Linley, J.E., K. Rose, M. Patil, B. Robertson, A.N. Akopian, and N. Gamper,** Inhibition of M current in sensory neurons by exogenous proteases: a signaling pathway mediating inflammatory nociception. *J Neurosci.* 28(44): p. 11240-9, 2008.
  29. **Liu, B., J.E. Linley, X. Du, X. Zhang, L. Ooi, H. Zhang, and N. Gamper,** The acute nociceptive signals induced by bradykinin in rat sensory neurons are mediated by inhibition of M-type K<sup>+</sup> channels and activation of Ca<sup>2+</sup>-activated Cl<sup>-</sup> channels. *J Clin Invest.* 120(4): p. 1240-52, 2010.
  30. **Liu, Y., H. Zhang, D. Huang, J. Qi, J. Xu, H. Gao, X. Du, N. Gamper, and H. Zhang,** Characterization of the effects of Cl(-) channel modulators on TMEM16A and bestrophin-1 Ca(2)(+) activated Cl(-) channels. *Pflugers Arch.* 467(7): p. 1417-30, 2015.
  31. **Lutter, D., F. Ullrich, J.C. Lueck, S. Kempa, and T.J. Jentsch,** Selective transport of neurotransmitters and modulators by distinct volume-regulated LRRC8 anion channels. *J Cell Sci.* 130(6): p. 1122-1133, 2017.
  32. **Manhas, N. and K.R. Pardasani,** Modelling mechanism of calcium oscillations in pancreatic acinar cells. *J Bioenerg Biomembr.* 46(5): p. 403-20, 2014.
  33. **Matolesi, M. and N. Giordano,** A novel explanation for observed CaMKII dynamics in dendritic spines with added EGTA or BAPTA. *Biophys J.* 108(4): p. 975-85, 2015.
  34. **Milenkovic, A., C. Brandl, V.M. Milenkovic, T. Jendryke, L. Sirianant, P. Wanitchakool, S. Zimmermann, C.M. Reiff, F. Horling, H. Schrewe, R. Schreiber, K. Kunzelmann, C.H. Wetzel, and B.H. Weber,** Bestrophin 1 is indispensable for volume regulation in human retinal pigment epithelium cells. *Proc Natl Acad Sci U S A.* 112(20): p. E2630-9, 2015.
  35. **Naraghi, M.,** T-jump study of calcium binding kinetics of calcium chelators. *Cell Calcium.* 22(4): p. 255-68, 1997.
  36. **Neher, E.,** Vesicle pools and Ca<sup>2+</sup> microdomains: new tools for understanding their roles in neurotransmitter release. *Neuron.* 20(3): p. 389-99, 1998.
  37. **Netti, V., A. Pizzoni, M. Perez-Dominguez, P. Ford, H. Pasantes-Morales, G. Ramos-Mandujano, and C. Capurro,** Release of taurine and glutamate contributes to cell volume regulation in human retinal Muller cells: differences in modulation by calcium. *J Neurophysiol.* 120(3): p. 973-984, 2018.
  38. **Nilius, B. and G. Droogmans,** Amazing chloride channels: an overview. *Acta Physiol Scand.* 177(2): p. 119-47, 2003.
  39. **Nilius, B., J. Eggermont, T. Voets, G. Buyse, V. Manolopoulos, and G. Droogmans,** Properties of volume-regulated anion channels in mammalian cells. *Prog Biophys Mol Biol.* 68(1): p. 69-119, 1997.
  40. **Okada, Y.,** Volume expansion-sensing outward-rectifier Cl<sup>-</sup> channel: fresh start to the molecular identity and volume sensor. *Am J Physiol.* 273(3 Pt 1): p. C755-89, 1997.
  41. **Okada, Y., K. Sato, and T. Numata,** Pathophysiology and puzzles of the volume-sensitive outwardly rectifying anion channel. *J Physiol.* 587(Pt 10): p. 2141-9, 2009.

42. **Ousingsawat, J., P. Wanitchakool, A. Kmit, A.M. Romao, W. Jantarajit, R. Schreiber, and K. Kunzelmann**, Anoctamin 6 mediates effects essential for innate immunity downstream of P2X7 receptors in macrophages. *Nat Commun.* 6: p. 6245, 2015.
43. **Parkash, J. and K. Asotra**, Calcium wave signaling in cancer cells. *Life Sci.* 87(19-22): p. 587-95, 2010.
44. **Pedersen, S.F., T.K. Klausen, and B. Nilius**, The identification of a volume-regulated anion channel: an amazing Odyssey. *Acta Physiol (Oxf)*. 213(4): p. 868-81, 2015.
45. **Pedersen, S.F., Y. Okada, and B. Nilius**, Biophysics and Physiology of the Volume-Regulated Anion Channel (VRAC)/Volume-Sensitive Outwardly Rectifying Anion Channel (VSOR). *Pflugers Arch.* 468(3): p. 371-83, 2016.
46. **Planells-Cases, R., D. Lutter, C. Guyader, N.M. Gerhards, F. Ullrich, D.A. Elger, A. Kucukosmanoglu, G. Xu, F.K. Voss, S.M. Reincke, T. Stauber, V.A. Blomen, D.J. Vis, L.F. Wessels, T.R. Brummelkamp, P. Borst, S. Rottenberg, and T.J. Jentsch**, Subunit composition of VRAC channels determines substrate specificity and cellular resistance to Pt-based anti-cancer drugs. *EMBO J.* 34(24): p. 2993-3008, 2015.
47. **Qiu, Z., A.E. Dubin, J. Mathur, B. Tu, K. Reddy, L.J. Miraglia, J. Reinhardt, A.P. Orth, and A. Patapoutian**, SWELL1, a plasma membrane protein, is an essential component of volume-regulated anion channel. *Cell.* 157(2): p. 447-458, 2014.
48. **Qu, Z. and H.C. Hartzell**, Functional geometry of the permeation pathway of Ca<sup>2+</sup>-activated Cl<sup>-</sup> channels inferred from analysis of voltage-dependent block. *J Biol Chem.* 276(21): p. 18423-9, 2001.
49. **Schreiber, R., D. Faria, B.V. Skryabin, P. Wanitchakool, J.R. Rock, and K. Kunzelmann**, Anoctamins support calcium-dependent chloride secretion by facilitating calcium signaling in adult mouse intestine. *Pflugers Arch.* 467(6): p. 1203-13, 2015.
50. **Schroeder, B.C., T. Cheng, Y.N. Jan, and L.Y. Jan**, Expression cloning of TMEM16A as a calcium-activated chloride channel subunit. *Cell.* 134(6): p. 1019-29, 2008.
51. **Stauffer, T.P., S. Ahn, and T. Meyer**, Receptor-induced transient reduction in plasma membrane PtdIns(4,5)P<sub>2</sub> concentration monitored in living cells. *Curr Biol.* 8(6): p. 343-6, 1998.
52. **Stuhlmann, T., R. Planells-Cases, and T.J. Jentsch**, LRRC8/VRAC anion channels enhance beta-cell glucose sensing and insulin secretion. *Nat Commun.* 9(1): p. 1974, 2018.
53. **Syeda, R., Z. Qiu, A.E. Dubin, S.E. Murthy, M.N. Florendo, D.E. Mason, J. Mathur, S.M. Cahalan, E.C. Peters, M. Montal, and A. Patapoutian**, LRRC8 Proteins Form Volume-Regulated Anion Channels that Sense Ionic Strength. *Cell.* 164(3): p. 499-511, 2016.
54. **Szucs, G., S. Heinke, G. Droogmans, and B. Nilius**, Activation of the volume-sensitive chloride current in vascular endothelial cells requires a permissive intracellular Ca<sup>2+</sup> concentration. *Pflugers Arch.* 431(3): p. 467-9, 1996.
55. **Ullrich, F., S.M. Reincke, F.K. Voss, T. Stauber, and T.J. Jentsch**, Inactivation and Anion Selectivity of Volume-regulated Anion Channels (VRACs) Depend on C-terminal Residues of the First Extracellular Loop. *J Biol Chem.* 291(33): p. 17040-8, 2016.
56. **Varnai, P. and T. Balla**, Visualization of phosphoinositides that bind pleckstrin homology domains: calcium- and agonist-induced dynamic changes and relationship to myo-[<sup>3</sup>H]inositol-labeled phosphoinositide pools. *J Cell Biol.* 143(2): p. 501-10, 1998.
57. **Voss, F.K., F. Ullrich, J. Munch, K. Lazarow, D. Lutter, N. Mah, M.A. Andrade-Navarro**,

- J.P. von Kries, T. Stauber, and T.J. Jentsch**, Identification of LRRC8 heteromers as an essential component of the volume-regulated anion channel VRAC. *Science*. 344(6184): p. 634-8, 2014.
58. **Yang, Y.D., H. Cho, J.Y. Koo, M.H. Tak, Y. Cho, W.S. Shim, S.P. Park, J. Lee, B. Lee, B.M. Kim, R. Raouf, Y.K. Shin, and U. Oh**, TMEM16A confers receptor-activated calcium-dependent chloride conductance. *Nature*. 455(7217): p. 1210-5, 2008.
59. **Zhang, Y., L. Xie, S.K. Gunasekar, D. Tong, A. Mishra, W.J. Gibson, C. Wang, T. Fidler, B. Marthaler, A. Klingelutz, E.D. Abel, I. Samuel, J.K. Smith, L. Cao, and R. Sah**, SWELL1 is a regulator of adipocyte size, insulin signalling and glucose homeostasis. *Nat Cell Biol*. 19(5): p. 504-517, 2017.
60. **Zholos, A., B. Beck, V. Sydorenko, L. Lemonnier, P. Bordat, N. Prevarskaya, and R. Skryma**, Ca(2+)- and volume-sensitive chloride currents are differentially regulated by agonists and store-operated Ca2+ entry. *J Gen Physiol*. 125(2): p. 197-211, 2005.

**Table 1 Characteristics of activation and inactivation of  $I_{Cl,swell}$  in HEK293 cells with different level of ANO1 and LRRC8A expression.**

	I/SS	Activation		Inactivation	
	(+100 mV)	$\tau 1$ (ms)	$\tau 2$ (ms)	$\tau 1$ (ms)	$\tau 2$ (ms)
WT	$2.90 \pm 0.26$	N/A	N/A	$37.62 \pm 5.86$	$506.7 \pm 67.2$
<i>ANO1</i> <sup>-/-</sup>	$4.29 \pm 0.43^{##}$	N/A	N/A	$38.78 \pm 7.62$	$290.9 \pm 13.4^{**}$
<i>LRRC8A</i> <sup>-/-</sup> + ANO1	$0.34 \pm 0.02^{##}$	$50.02 \pm 9.12$	$283.8 \pm 62.4$	N/A	N/A
<i>LRRC8A</i> <sup>-/-</sup> + LRRC8A	$1.52 \pm 0.09^{##}$	N/A	N/A	$606.6 \pm 99.1(\tau)$	

I/SS, the ratio of instantaneous and pseudo steady state current amplitudes measured at +100 mV. All values are means  $\pm$  S.E.M (n = 6-11). N/A, not available

\*\* $P < 0.01$ , ## $P < 0.01$ , compared with current recorded in WT HEK293 cells.

**Table 2 Inhibition effects of NFA and DCPIB on  $I_{Cl,swell}$  and CaCC currents measured at -60 mV and +100 mV.**

NFA	DCPIB
IC <sub>50</sub> ( $\mu$ M)	IC <sub>50</sub> ( $\mu$ M)

	-60 mV	+100 mV	-60 mV	+100 mV
CaCC/ANO1	N/A	3.35 ± 1.87	27.7 ± 3.96	18.8 ± 2.71
I <sub>Cl,swell</sub>	740.2 ± 78.4	471.4 ± 132.8	6.34 ± 1.45	5.69 ± 1.6
I <sub>Cl,swell</sub> + ANO1	220.4 ± 44.1	95.8 ± 15.6	7.75 ± 1.56	7.04 ± 2.29

All values are means ± S.E.M (n = 4-16). N/A, no activity.

I<sub>Cl,swell</sub> were induced by the hypertonic intracellular solution in HEK293 cells (I<sub>Cl,swell</sub>), or in HEK293 cells over-expressing ANO1 (I<sub>Cl,swell</sub> + ANO1); CaCC currents were induced by isotonic intracellular solution containing high Ca<sup>2+</sup> (447 nM) in CHO cells stably expressing ANO1.

## Figure legends

### **Fig. 1. Local $\text{Ca}^{2+}$ plays an essential role in activation of VRACs.**

The cells were continuously held at -60 mV and stimulated with 1 s voltage ramps from -100 mV to +100 mV applied with 60s interval; to measure current-voltage relationships voltage steps from -100 mV to +100 mV in 20 mV increments were applied instead of the ramps. The dotted lines indicate the zero current level. *A*: top, volume regulated chloride current ( $I_{\text{Cl,swell}}$ ) recorded in HEK293 cell elicited by 420 mOsm hypertonic pipette solution. Bottom, the representative current traces induced by ramp (left) and step (right) voltage protocols, respectively. In the top panel, the times at which ramp- and step-induced I/V relationships were obtained are indicated by numbers (1, 2) and asterisk, respectively. DCPIB (10  $\mu\text{M}$ ) was applied at the end of the recording during the time indicated by grey shading. *B*: top and middle, representative current traces of  $I_{\text{Cl,swell}}$  induced by the hypertonic pipette solution with 20 mM EGTA or 20 mM BAPTA, as indicated. Bottom, representative current traces of  $I_{\text{Cl,swell}}$  induced by the hypertonic pipette solution in HEK293 cells treated with 2  $\mu\text{M}$  thapsigargin; thapsigargin was applied 15 min before and was perfused continuously during the experiment. *C*: summary data for maximal current densities of  $I_{\text{Cl,swell}}$  (recorded at -60 mV) from experiments presented in panels (A and B).  $**P < 0.01$ , compared with the control HEK293 cells. *D* and *E*: summary data for maximal current densities of  $I_{\text{Cl,swell}}$  (recorded at -60 mV) from ANO1 stably-transfected CHO cells and DRG neurons.  $**P < 0.01$ , compared with the control cells.

### **Fig. 2. No effects of extracellular $\text{Ca}^{2+}$ on $I_{\text{Cl,swell}}$ or intracellular $\text{Ca}^{2+}$ transients.**

The HEK293 cells were continuously held at -60 mV and stimulated with 1 s voltage ramps from -100 mV to +100 mV applied with 60s interval; to measure current-voltage relationships voltage steps from -100 mV to +100 mV in 20 mV increments were applied instead of the ramps. The dotted lines indicate the zero current level. *A*: representative current traces of  $I_{\text{Cl,swell}}$  induced by 220 mOsm

hypotonic bath solution in the absence or presence of EGTA. *B*: representative current traces of  $I_{Cl,swell}$  induced by the hypotonic bath solution with 20 mM EGTA or 20 mM BAPTA in the 320 mOsm isotonic pipette solution, as indicated. *C* and *D*: intracellular  $Ca^{2+}$  transients recorded with Fluo-4-AM (2  $\mu$ M). Time courses of Fluo-4 fluorescence intensity from three HEK293 cells indicated by the arrowheads in the insets on the left; insets depict cells before (a) and during (b) application of the hypotonic bath solution (220 mOsm) in the absence (*C*) or presence (*D*) of EGTA. *E* and *F*: summary data for maximal current densities of  $I_{Cl,swell}$  (recorded at -60 mV) from experiments presented in panels (*A* and *B*). \*\*\* $P < 0.001$ , compared with the control HEK293 cells. *G*: summary for the maximal change in Fluo-4 fluorescence intensity (normalized to the initial fluorescence intensity,  $F_0$ ) during the first transient induced by hypotonic bath solution in the absence or presence of EGTA (from the experiments as these shown in the panels (*C* and *D*), respectively. In (*E-G*), number of recordings in more than 3 sets of experiments is indicated within each bar.

**Fig. 3. Local  $Ca^{2+}$  is essential for activation of LRRC8A currents.**

*A*: overexpression of LRRC8A in HEK293 cells lacking endogenous LRRC8A (*LRRC8A*<sup>-/-</sup>) rescued  $I_{Cl,swell}$  elicited by 420 mOsm hypertonic pipette solution. *B*: BAPTA and thapsigargin (Thap) were more efficient than EGTA in preventing activation of LRRC8A currents. In (*A* and *B*) the recording conditions are similar to the experiments shown in Figure 1. Where indicated by grey shading, 10  $\mu$ M DCPIB was applied at the end of the recording. *C*: summary data for experiments exemplified in (*A*), maximal current densities were measured at -60 mV. \*\* $P < 0.01$ , compared with current recorded in WT HEK293 cells. *D*: summary data for experiments exemplified in (*B*), maximal current densities were measured at -60 mV. \*\*\* $P < 0.001$ , compared with the control *LRRC8A*<sup>-/-</sup> cells transfected with LRRC8A. In (*C* and *D*), number of recordings in more than 3 sets of experiments is indicated within each bar.

**Fig. 4. Overexpressed ANO1, but not LRRC8A, is activated by cytosolic  $Ca^{2+}$**

## dialysis.

*A-C*: WT HEK293 cells (*A*), *LRRC8A*<sup>-/-</sup> HEK293 cells transfected with LRRC8A (*B*) and HEK293 cells transfected with ANO1 (*C*), were perfused with a pipette solution contained 447 nM free Ca<sup>2+</sup> and the whole-cell currents were recorded using the ramp voltage protocol shown at the top right inset in (*A*). The osmolality of the pipette solution was an isotonic (320 mOsm). *D*: summarized maximal current densities measured at -60 mV and +100 mV from the experiments exemplified in panels (*A-C*). \*\**P* < 0.01, ##*P* < 0.01 compared with WT HEK293; number of recordings in more than 3 sets of experiments is indicated under the bars.

## **Fig. 5. ANO1 is activated by cell swelling and contributes to VRAC.**

*A-C*: left,  $I_{Cl,swell}$  recorded in HEK293 lacking ANO1 (HEK293 *ANO1*<sup>-/-</sup>), HEK293 transfected with ANO1 (HEK293-ANO1) and HEK293 *LRRC8A*<sup>-/-</sup> transfected with ANO1;  $I_{Cl,swell}$  was elicited with 420 mOsm hypertonic pipette solution and recorded as in Figure 1. Right, the representative current traces induced by step protocol (top inset) at the times indicated by asterisks. *D*: summary data for experiments exemplified in (*A*), maximal current densities were measured at -60 mV, \*\**P* < 0.01, \*\*\**P* < 0.001 compared with the current recorded in HEK293 cells. *E*: summary data for experiments exemplified in (*C*), maximal current densities were measured at -60 mV and +100 mV. \*\**P* < 0.01, ##*P* < 0.01 compared with the current recorded in *LRRC8A*<sup>-/-</sup> cells at -60 mV and +100 mV, respectively. *F* and *G*: representative current traces recorded from HEK293 cells (*F*) and *LRRC8A*<sup>-/-</sup> HEK293 cells transfected with ANO1 (*G*). Currents were elicited by the dialysis of isotonic (320 mOsm) pipette solution containing 200 μM GTP-γs. DCPIB (10 μM) was applied at the end of the recording during the time indicated by grey shading. *H*: Summary data for current densities of  $I_{Cl,swell}$  from experiments presented in panel (*F* and *G*). \*\**P* < 0.01 compared with HEK293 cells at -60 mV. ##*P* < 0.01 compared with HEK293 cells at +100 mV.

**Fig. 6. Genetic deletion of either ANO1 or LRRC8A did not affect the  $I_{Cl,swell}$  and intracellular  $Ca^{2+}$  transients induced by a hypotonic extracellular solution.**

*A* and *B*: BAPTA but not EGTA prevented activation of  $I_{Cl,swell}$  in HEK293 cells lacking ANO1. In some experiments, 10  $\mu$ M DCPIB was applied at the end of the recording during the time indicated by grey shading. *C* and *D*: genetic deletion of either ANO1 or LRRC8A did not affect the intracellular  $Ca^{2+}$  transients induced by a hypotonic extracellular solution. *E*: summary data for current densities of  $I_{Cl,swell}$  from experiments presented in panel (*A* and *B*). \*\*\* $P < 0.001$  compared with ANO1 lacking HEK293 cells at -60 mV. *F*: summary for the maximal change in normalized Fluo-4 fluorescence intensity during the first transient induced by hypotonic bath solution in experiments as those shown in (*C* and *D*).

**Fig. 7. Effects of  $Cl^-$  channel inhibitors on  $I_{Cl,swell}$  and CaCC currents.**

*A*: representative current traces induced by voltage ramps from -100 to +100 mV (from a holding potential of -60 mV) during the application of different concentrations (as indicated) of NFA and DCPIB.  $I_{Cl,swell}$  was induced with 420 mOsm hypertonic intracellular solution in WT HEK293 cells;  $I_{Cl,swell} + ANO1$  was induced with 420 mOsm hypertonic intracellular solution in HEK293 cells stably transfected with ANO1 (HEK293-ANO1); and CaCC/ANO1 was induced with high free  $Ca^{2+}$  (447 nM) isotonic intracellular solution in HEK293-ANO1 cells. *B*: NFA and DCPIB selectively inhibited different components of  $I_{Cl,swell}$  in HEK293-ANO1 cells. Currents were recorded using step voltage protocol (Figure. 1(A)). NFA and DCPIB sensitive current fractions were obtained by subtracting residual currents in the presence of a drug from the total  $I_{Cl,swell}$  before drug application. *C* and *D*: NFA and DCPIB concentration-response relationships for three different currents recorded at +100 mV. The data were fitted with a logistic function; the  $IC_{50}$  values are shown.

**Fig. 8. PLC isoforms are required for the  $I_{Cl,swell}$  activation.**

*A*:  $I_{Cl,swell}$  elicited by the hypertonic pipette solution containing 20 mM EGTA was

blocked by the PLC blocker, U73122 (5  $\mu$ M; upper trace) but not by the inactive analogue, U73343 (5  $\mu$ M; lower trace). HEK293 cells were pre-treated with either of the drug for 20 min; the drugs were also present in extracellular solution during the recording. CaCC<sub>inh</sub>-A01 (100  $\mu$ M) was applied at the end of the recording during the time indicated by grey shading. *B*: summary data for experiments exemplified in the panel (A). \*\* $P < 0.01$ , compared with the control HEK293 cells. *C*: efficiency of PLC-siRNAs knockdown (as indicated) on HEK293 cells. The scrambled siRNA control and siRNA against PLC isoforms were transfected into HEK293 cells 72 h before tested using Real time PCR approach. *D*: summary data for effect of siRNA against different PLC isoforms on  $I_{Cl,swell}$  recorded at the holding potentials of -60 mV. \*\* $P < 0.01$ , compared with scrambled siRNA.

Figure 1

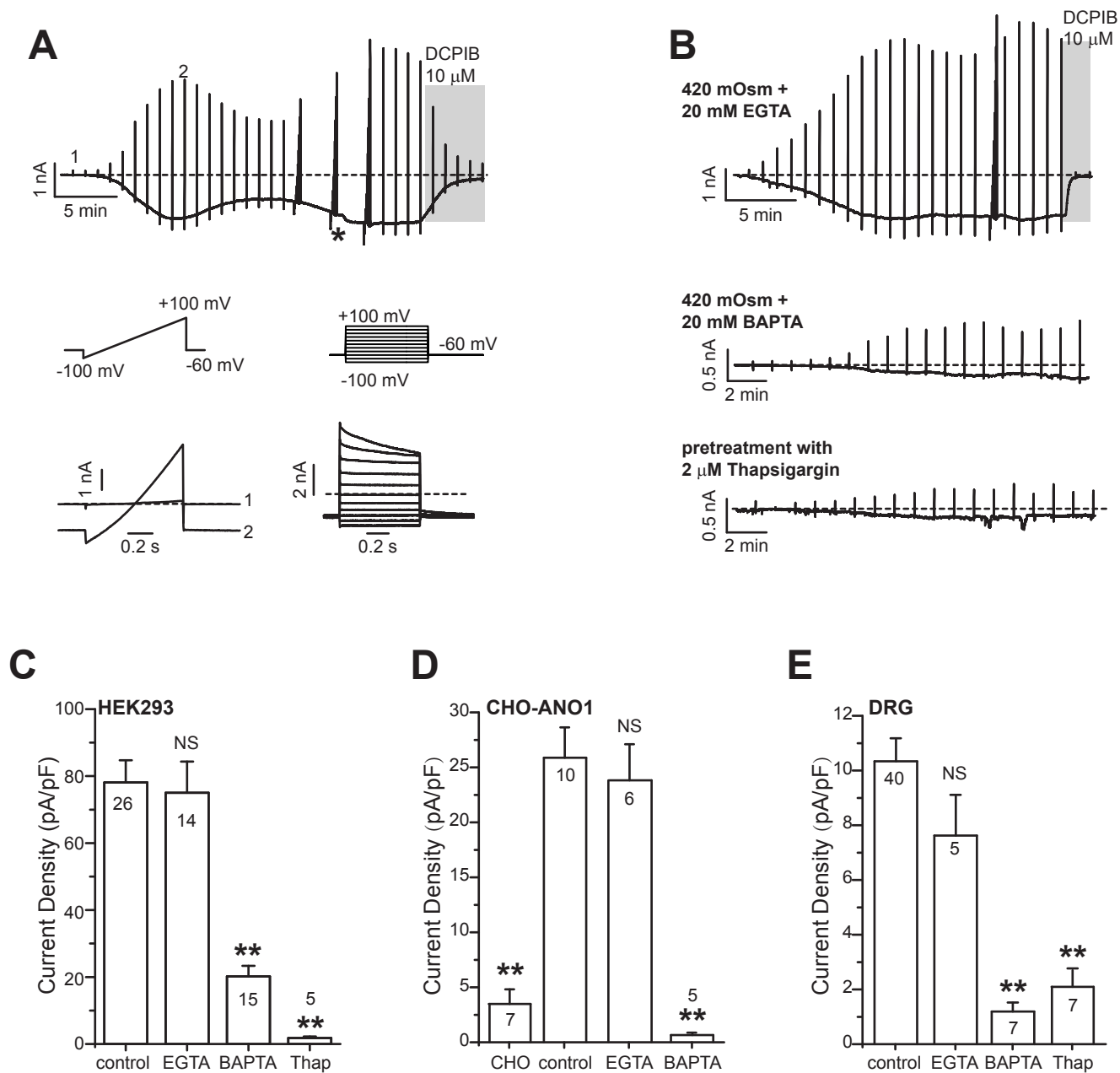


Figure 2

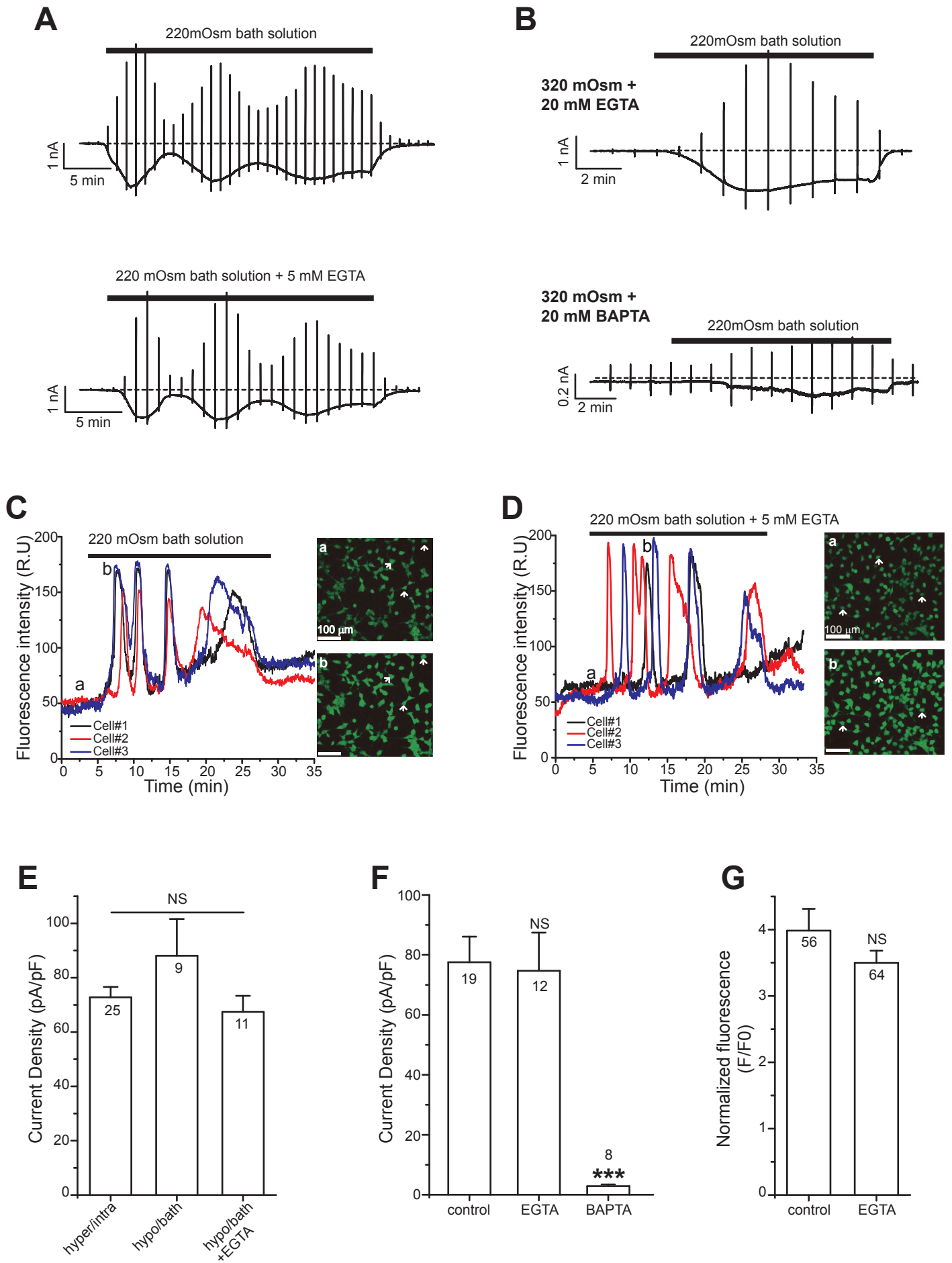
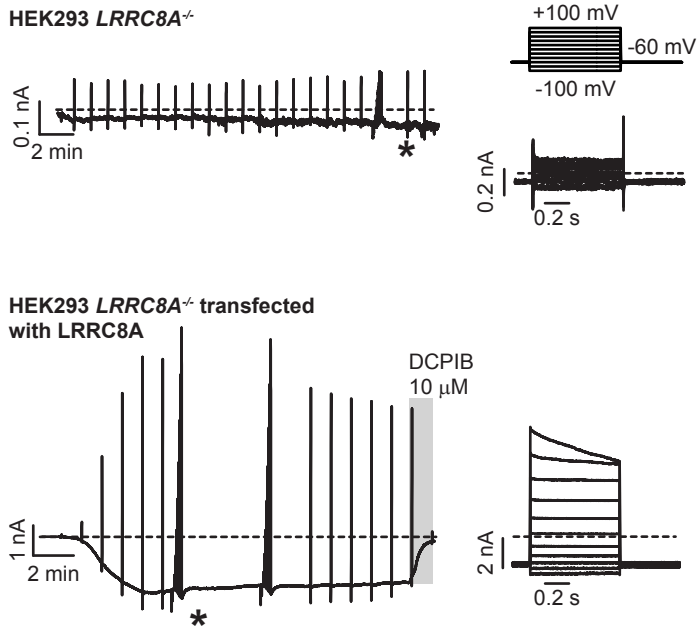
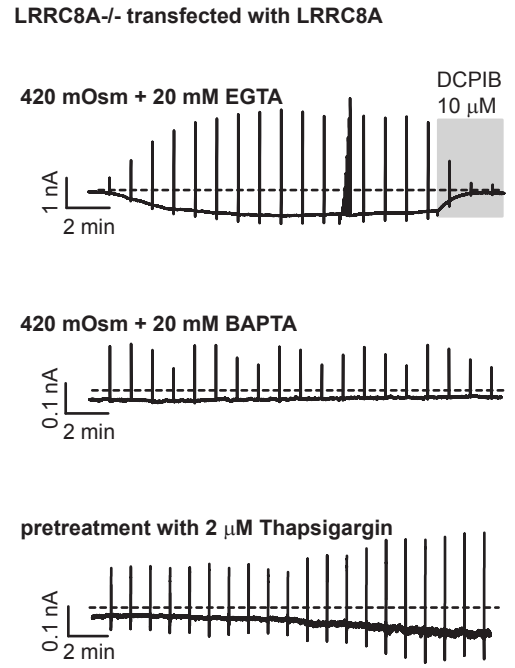


Figure 3

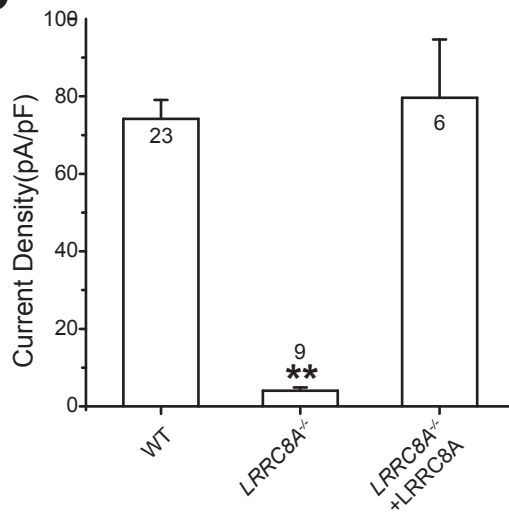
**A**



**B**



**C**



**D**

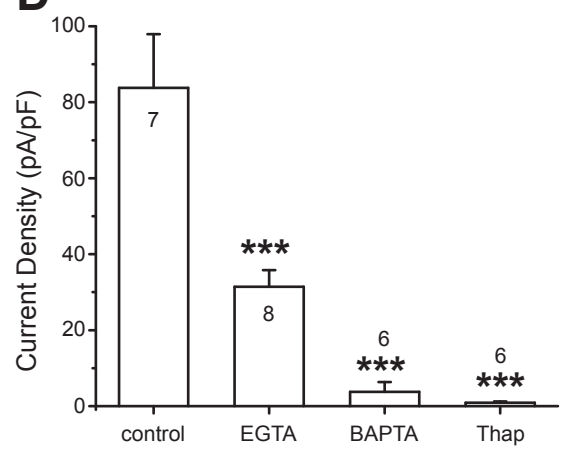


Figure 4

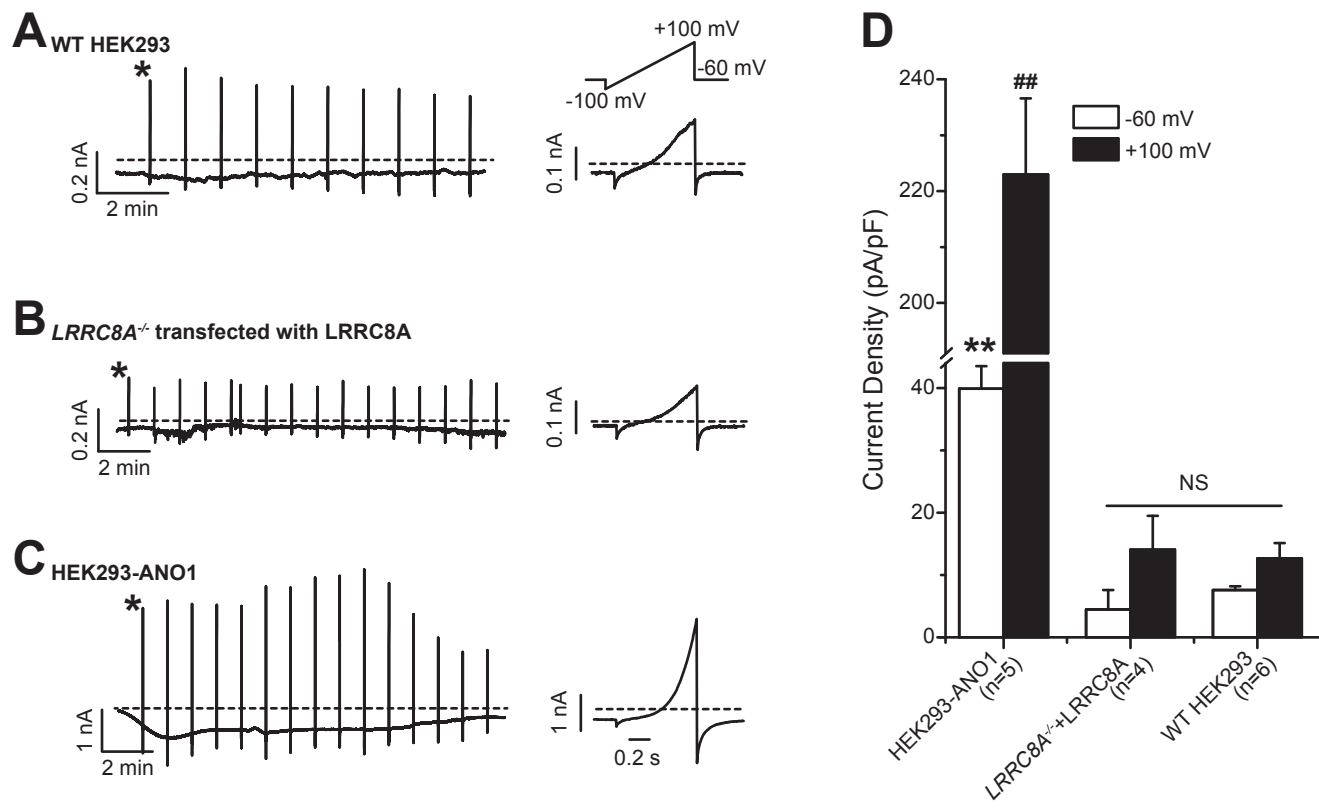
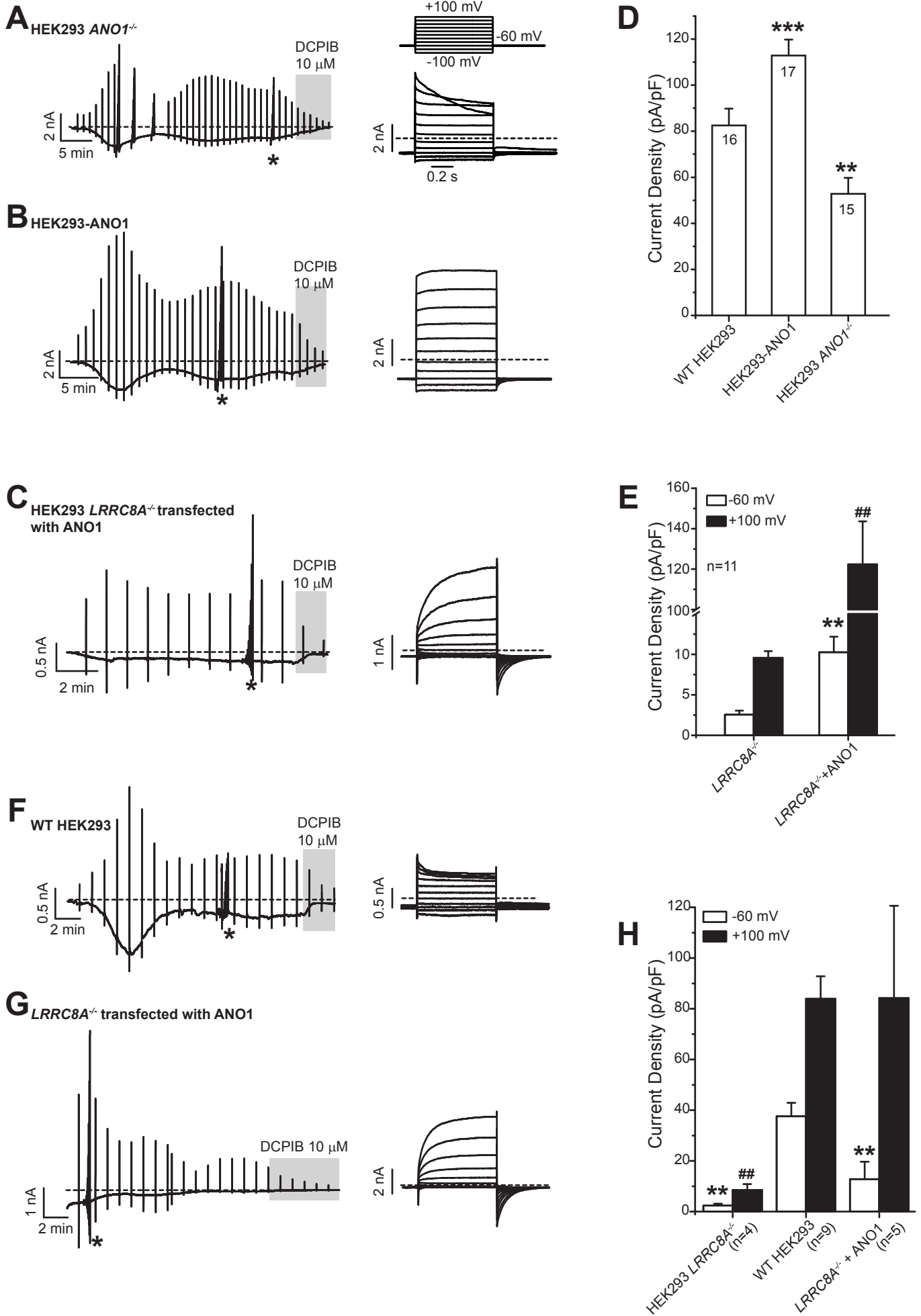


Figure 5



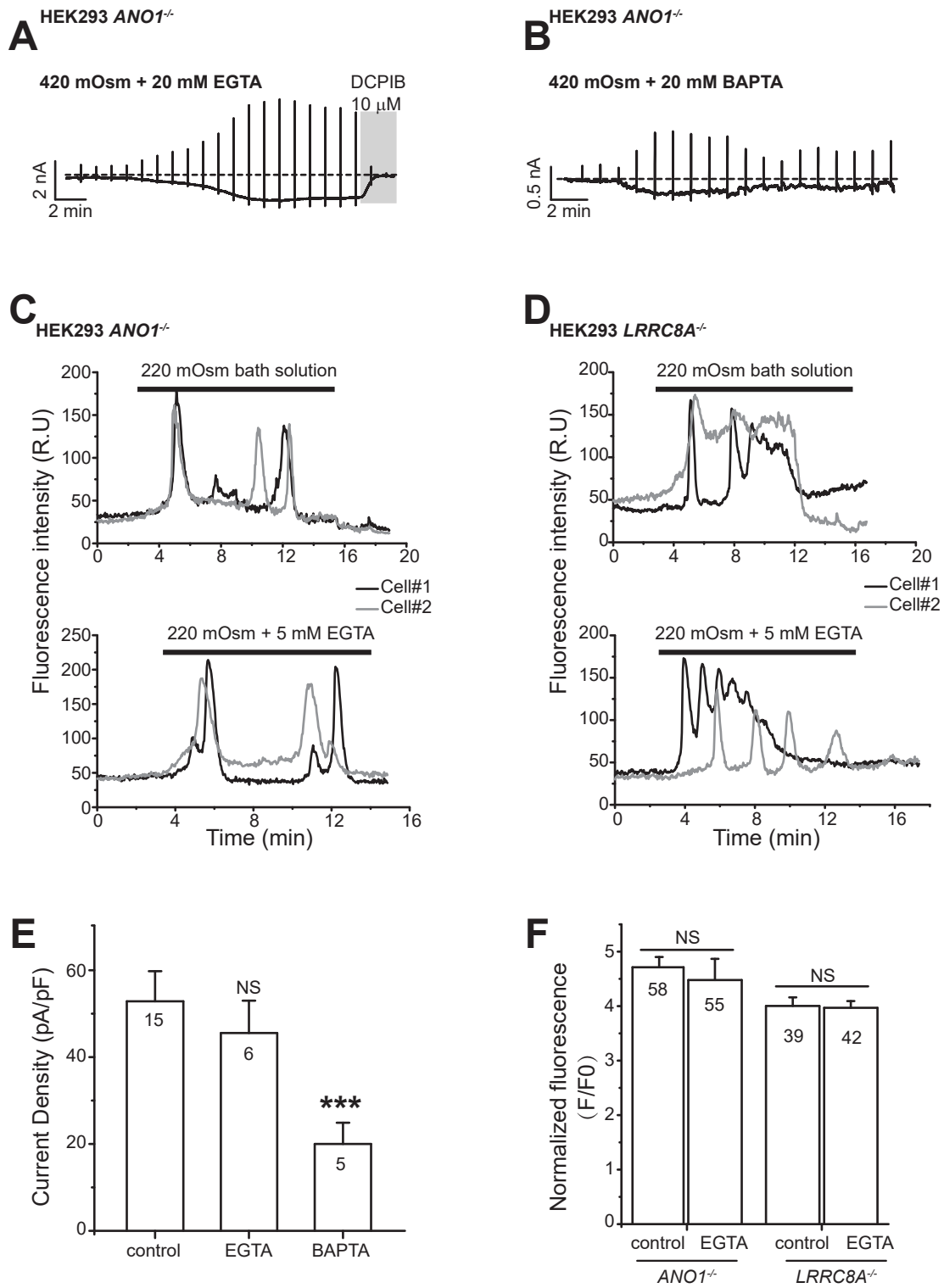


Figure 7

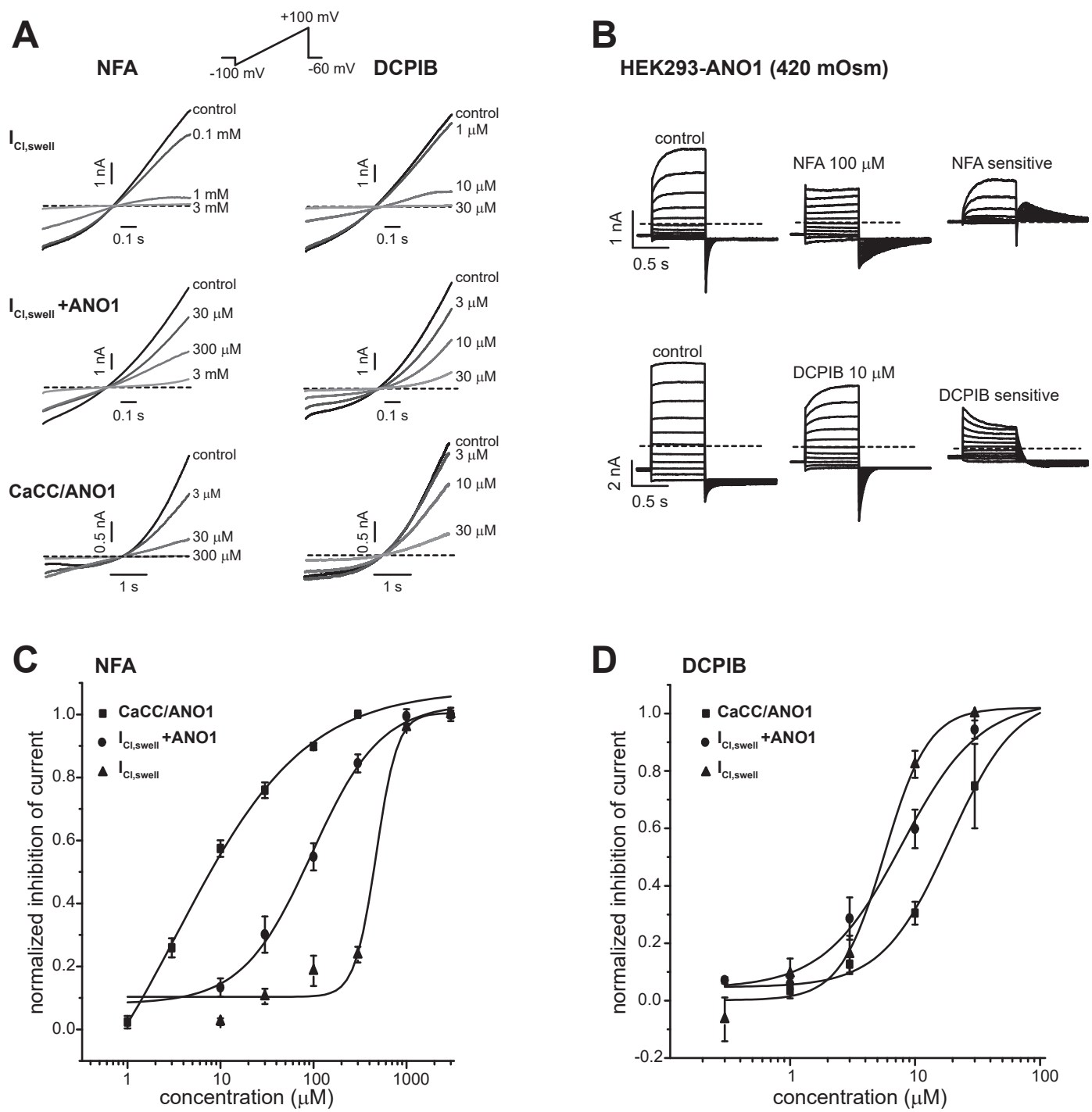
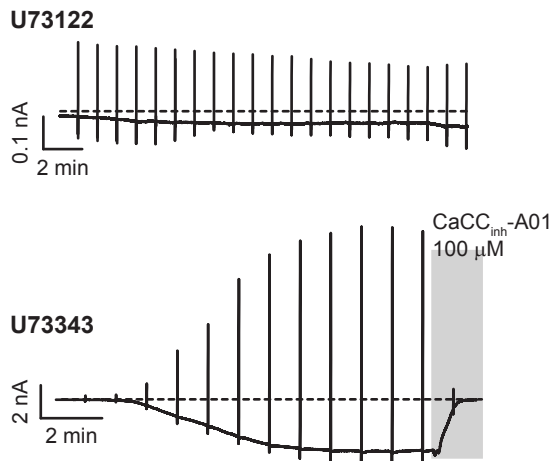
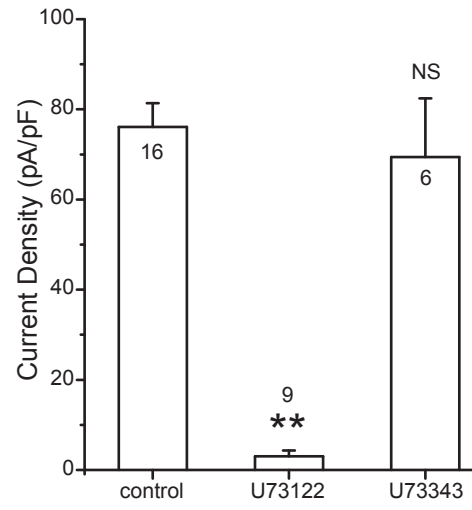


Figure 8

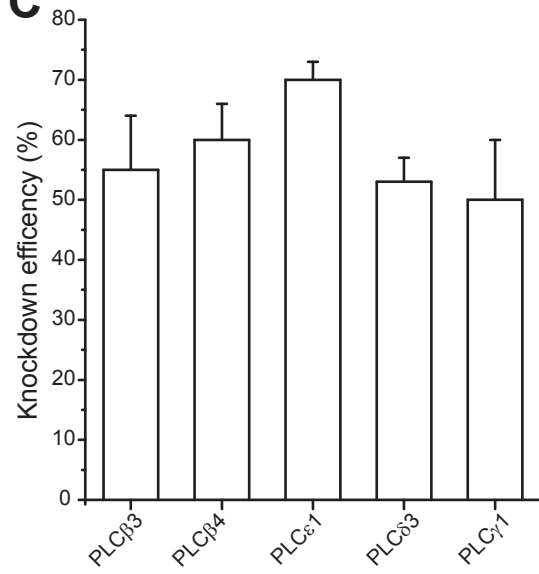
**A**



**B**



**C**



**D**

